VOL. 16 No. 4, pp. 105-140 OCTOBER 1954

Philips Technical Review

DEALING WITH TECHNICAL PROBLEMS
RELATING TO THE PRODUCTS, PROCESSES AND INVESTIGATIONS OF
THE PHILIPS INDUSTRIES

EDITED BY THE RESEARCH LABORATORY OF N.V. PHILIPS' GLOEILAMPENFABRIEKEN, EINDHOVEN, NETHERLANDS

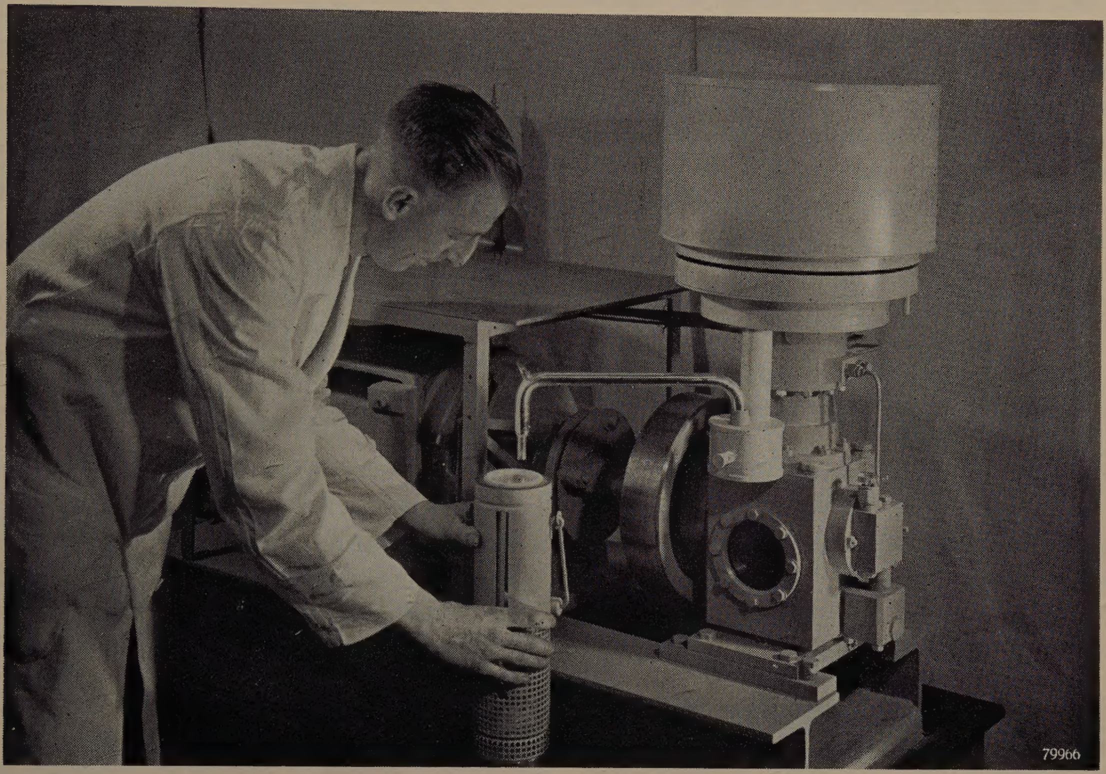

CONSTRUCTION OF A GAS REFRIGERATING MACHINE

by J. W. L. KÖHLER and C. O. JONKERS.

621.573

A theoretical study of the gas refrigeration cycle, recently published in this Review, was based on research in the Philips laboratories in Eindhoven closely parallel to work on the hot-gas engine. The present article deals with the application of this cycle and describes a practical machine for its realization. The results achieved with this machine will be discussed, especially with a view to possible applications of this new refrigeration cycle.

For the practical application of the gas refrigeration cycle — the principles of which were discussed in the previous issue of this Review [1] — a number of problems have first to be solved. Before discussing these problems it may be useful to recapitulate briefly the principle of the gas refrigeration cycle.

A quantity of gas is compressed at room temperature, after which it is cooled to a low temperature. At this temperature it is permitted to expand and the cold thus produced is utilized. After the expansion, the gas is re-heated to room temperature, and the cycle is completed. The cooling and re-heating of the gas takes place by an exchange of heat in a regenerator. The working fluid is at all times in the gaseous state and will be considered here as a perfect gas.

---

[1] J. W. L. Köhler and C. O. Jonkers, Fundamentals of the gas refrigerating machine, Philips tech. Rev. **16**, 69-78, 1954/55 (No. 3), hereafter referred to as I.

As mentioned in I, it has been found in the course of research that machines based on this principle have the most favourable properties when used to produce cold between —80 °C and —200 °C. The existence of this optimum range, however, cannot be derived from the discussion of the idealized process in I. This follows from the fact that the efficiency of the ideal cycle (no losses) is at all temperatures equal to that of a Carnot cycle working within the same temperature limits; *as regards efficiency therefore, the ideal process cannot be surpassed at any temperature.* The provision that the working fluid must behave as a perfect gas to a sufficient approximation, does not constitute a restriction even at —200 °C, for it can be satisfied by using hydrogen or helium even at considerably lower temperatures.

Limitations of the process

It has been found that the limitation of the process to the above temperature range for efficient working is due to deviations from the ideal cycle which occur in practice. They result in an increase of the required shaft power and a decrease in the refrigerating capacity; the smaller the values of these quantities, the more serious are the relative effects of the losses. *Fig. 1* shows that we may expect that *increase of the required shaft power limits the process at high temperature while decrease of the refrigerating capacity limits it at low temperature.* In this way we arrive at the aforementioned temperature range, i.e. the optimum working range, in which the actual efficiency differs least from the ideal efficiency — see *fig. 2.* The limits of this range are not fixed precisely, since they greatly depend on present and future technological possibilities. We shall now examine in more detail these deviations from ideal behavior which give rise to the optimum range.

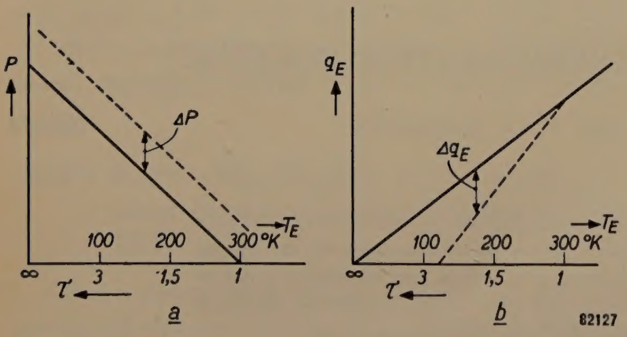

Fig. 1. Graphs of the shaft power P and the refrigerating capacity q_{E} of the gas refrigerating machine as functions of the temperature ratio $\tau = T_{\mathrm{C}}/T_{\mathrm{E}}$ (T_{C} = temperature of the cooler $\approx$ 300 °K, T_{E} = the desired low temperature). The full lines apply to the ideal machine (see fig. 10 in I), the dotted line to a practical machine subject to various losses.

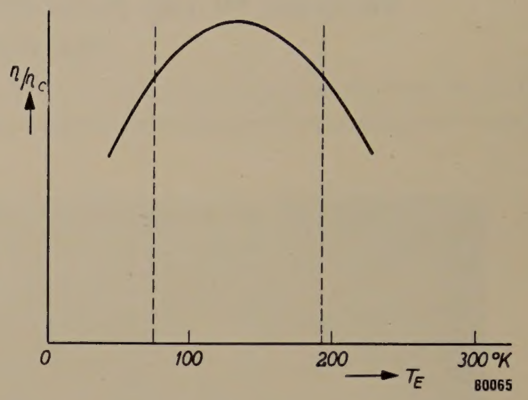

Fig. 2. The "figure of merit" η/η_c of the gas refrigerating machine as a function of the temperature (η = efficiency of the actual machine, η_c = Carnot-efficiency, cf. I). The diagram shows how the influence of the losses limits the useful temperature range of the machine.

Losses increasing the shaft power

The drive of every machine is subject to frictional losses, so that a certain amount of extra power is required merely to keep the machine going. In the gas refrigerating machine the absolute value of this "mechanical loss" is practically independent of the freezing temperature [2]), as may be seen from the dotted curve in fig. 1*a*; the relative effect of this loss is therefore greatest at a high temperature.

Another effect of a similar character to the mechanical loss is what is termed the "adiabatic loss". In I it was assumed that in the cylinders the heat transfer between the gas and the surrounding walls is so complete that the heat of compression and the cold of expansion can be discharged during every phase of the process. This, however, is very difficult to realize. For this reason heat exchangers have been incorporated between the cylinders and the regenerator (a "cooler" at the compression side and a "freezer" at the expansion side), which establish the thermal contact between the interior of the machine and the outside. In these heat exchangers the refrigerant gas is caused to flow through narrow channels, so that a good thermal contact with the walls is attained.

If we assume the thermal contact in these heat exchangers to be perfect, then we obtain a situation as shown in *fig. 3*, in which the temperatures of the various parts of the machine have been indicated schematically. The temperature of the cooler is determined by the temperature of the cooling water, and the freezer temperature by the temperature at which the cold is to be utilized, e.g. the boiling point of air. The gas enters the cylinders at the temperature of the heat exchangers; after this the gas temperature varies adiabatically with the pressure inside the machine. This means that the average temperature T_{Ca} in the compression cylinder will be higher than the temperature T_{C} of the cooler (due to compression of the gas), whilst the average temperature T_{Ea} of the expansion cylinder will be lower than T_{E}.

---

[2]) The pressure ratio, which determines the forces and hence the losses set up in the drive, is in fact, only slightly influenced by the freezing temperature. Incidentally it is to be noted in this connection that in the compression refrigerator the mechanical losses will increase as the evaporator temperature decreases.

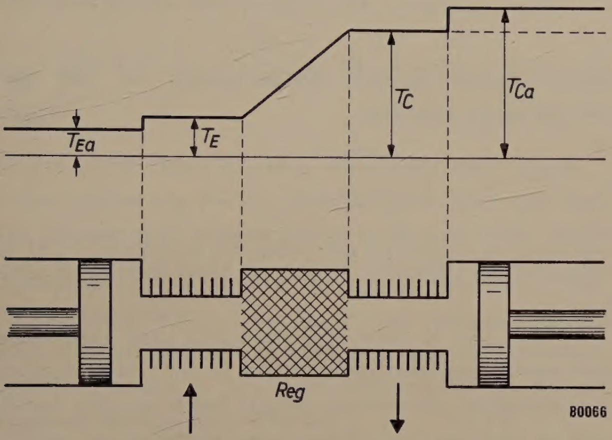

Fig. 3. Temperature distribution in the gas refrigerating machine. The machine is equipped with two heat exchangers effecting the thermal contact between the refrigerant and the ambient atmosphere. The first (the "freezer") is at the low temperature T_{E}, the second (the "cooler") is at room temperature T_{C}. Between the two, in the regenerator (*Reg*), there is a gradual transition between the two values. The two arrows indicate the direction of flow of heat in the two cases.

Owing to the adiabatic behaviour of the refrigerant in both the expansion and the compression cylinder, the average temperature T_{Ea} in the former is slightly lower than T_{E}, whilst the average temperature T_{Ca} in the latter is slightly higher than T_{C}. This is the cause of the "adiabatic loss".

We then see that $T_{\mathrm{Ca}}/T_{\mathrm{Ea}} = \tau_{\mathrm{a}} > \tau$, which means that the machine works internally at a greater temperature ratio than externally. From fig. 1*a* it can be concluded that the shaft power is then greater than in the isothermal case. It can be shown very simply that the value of this additional shaft power is very little influenced by the freezing temperature, so that the effect of this loss, as for frictional losses in the drive, is relatively greater at high temperatures.

By analogy with the expression derived for the shaft power in the isothermal process, $P_{\mathrm{iso}} = q_{\mathrm{E}}\,(\tau-1)$, (cf. I, eq. 14), we can put:

$$P_{\mathrm{a}} \approx q_{\mathrm{E}}(\tau_{\mathrm{a}}-1).$$

The value of the refrigerating capacity q_{E} is found to be practically the same for both processes, owing to the fact that the decrease due to the greater temperature ratio, as would be expected according to fig. 1*b*, is compensated by the greater pressure ratio inherent in the adiabatic process. The additional shaft power thus amounts to:

$$\Delta P_{\mathrm{a}} = P_{\mathrm{a}} - P_{\mathrm{iso}} \approx q_{\mathrm{E}}\,(\tau_{\mathrm{a}}-\tau) = q_{\mathrm{E}}\,\tau\,(\frac{\tau_{\mathrm{a}}}{\tau}-1).$$

The ratio τ_{a}/τ depends very little on the freezing temperature T_{E}, because the pressure ratio changes very little with the temperature; we can therefore put:

$$\frac{\tau_{\mathrm{a}}}{\tau} \approx 1+\beta,$$

where β is independent of T_{E}. Consequently

$$\frac{\Delta P}{P_{\mathrm{iso}}} \approx \frac{q_{\mathrm{E}}\tau\beta}{q_{\mathrm{E}}(\tau-1)} = \frac{\beta T_{\mathrm{C}}}{T_{\mathrm{C}}-T_{\mathrm{E}}}.$$

This makes it clear that the relative effect of adiabatic loss is greatest when T_{E} differs least from T_{C}.

The adiabatic loss is approximately proportional to the pressure ratio. It can therefore be limited by reducing the pressure ratio. This, however, impairs the refrigerating capacity, so that it must not be carried too far.

Losses reducing the refrigerating capacity

The cold parts of the machine can never be completely protected against loss of cold (or influx of heat) through conduction. The lower the freezing temperature, the greater becomes the influence of this "insulation loss".

If G is the thermal conductivity of the particular section causing the loss, then the loss of cold per unit time amounts to;

$$\Delta q_{\mathrm{G}} = G(T_{\mathrm{C}} - T_{\mathrm{E}}) \quad . \; . \; . \; . \; . \; . \; . \quad (1)$$

This loss should be compared with the refrigerating capacity q_{E}, which is approximately proportional to T_{E}, i.e. $q_{\mathrm{E}} \approx CT_{\mathrm{E}}$. Hence

$$\frac{\Delta q_{\mathrm{G}}}{q_{\mathrm{E}}} \approx \frac{G}{C}\frac{T_{\mathrm{C}}-T_{\mathrm{E}}}{T_{\mathrm{E}}} = \frac{G}{C}\,(\tau-1). \quad . \; . \; . \quad (2)$$

The relative influence of the insulation loss at very low temperatures is therefore practically inversely proportional to the freezing temperature T_{E} (cf. the dotted line in fig. 1*b*); this effect is mainly due to the decrease of the refrigerating capacity with T_{E}.

The insulation losses through conduction play only a minor part in the gas refrigeration machine, as the cold parts can be built compactly. The losses caused by a non-perfect regenerator, however, will also have the character of insulation losses, and it is these losses that are more difficult to combat. *This "regeneration loss" is the major limitation of the refrigerating capacity at very low temperatures* It can be roughly estimated as follows:

The quantity of heat Q_r which the gas has to discharge on its way from the compression space to the expansion space, is stored in the mass of the regenerator. For this a loosely packed mass of thin wire is used. This mass of wire shows a continuous temperature change in the direction of the gas flow; the form of this temperature distribution is roughly represented in fig. 3.

The value of Q_r is given by the equation

$$Q_r = W_g(T_C - T_E), \quad . \; . \; . \; . \; . \quad (3)$$

where W_g represents the thermal capacity of the gas flowing through the regenerator per half cycle. In practice, however, slightly less than the full amount of heat Q_r is transferred to the regenerator mass, viz. $\eta_r Q_r$, η_r being the efficiency of the regenerator ($\eta_r = 1$ for ideal regeneration). The difference between Q_r and $\eta_r Q_r$, which is denoted by ΔQ_r, is the regeneration loss:

$$\Delta Q_r = Q_r - \eta_r Q_r = (1-\eta_r)\, W_g\, (T_C - T_E), \quad (4)$$

or, per second:

$$\Delta q_r = w_g\, (1-\eta_r)\, (T_C - T_E), \quad . \; . \; . \quad (4a)$$

where w_g represents $nW_g/60$, and n is the number of r.p.m. of the machine.

This regeneration loss wastes part of the cold produced and thus reduces the refrigerating capacity. If we compare (4a) with (1), we notice that the regeneration loss has formally the character of an insulation loss if $(1-\eta_r)w_g$ is considered as the thermal conductivity of the regenerator.

The relative regeneration loss now becomes:

$$\frac{\Delta q_r}{q_E} \approx \frac{w_g}{C}\,(1-\eta_r)\,\frac{T_C - T_E}{T_E} = \frac{w_g}{C}\,(1-\eta_r)\,(\tau - 1). \quad (5)$$

w_g/C is very little dependent on T_E; its value is approximately 7. The following *table*, computed for a value of $\eta_r = 0.99$ (which can actually be obtained in practice), shows the influence of the regeneration loss in various cases).

Temperature range	T_E in °K	$\frac{\Delta q_r}{q_E}$ in %
liquid air	75	21
liquid hydrogen	20	98
hot-gas engine	900	4.7

At the boiling point of air the loss (21%) is acceptable. At 20° K, however, the loss has risen to 98%, so that the refrigerating capacity is almost completely vitiated by the regeneration loss. For comparison, the value for the hot-gas engine has also been given; this shows that there the regeneration problem is less important than in the refrigerator.

There are two main factors which cause the efficiency of regenerators to deviate from unity, viz, imperfect heat transfer between the gas and the regenerator mass and the finite heat capacity of this mass. Because of the imperfect heat transfer the gas will not exactly follow the temperature of the regenerator mass, so that it is not cooled down or warmed up to the correct temperature. Because of the finite heat capacity of the regenerator, its temperature changes while the gas flows through it; this has the same effect.

The relationship between heat transfer, heat capacity and the efficiency of regenerators has been dealt with by *Hausen* [3]).

Miscellaneous losses: dimensioning of the gas refrigerating machine

Apart from the losses already dealt with, which limit the field of application of the gas refrigeration cycle, there are some other causes that impair the efficiency in practice, which we shall briefly discuss now.

In fig. 3 it is explicitly assumed that the cooler and the freezer are ideal. If this is not the case, then temperature differences occur, both at the inside and at the outside of the heat exchangers, and in addition, a temperature difference arises between inside and outside, owing to the thermal resistance of the material of the heat exchanger. In this way the gas temperature in the cooler becomes higher and that in the freezer lower than required, so that the machine has to operate internally at a higher temperature ratio. This loss is somewhat similar to the adiabatic loss, though of less importance [4]).

Consequently, in designing a gas refrigerating machine, the aim will be to attain the largest possible transfer of heat in cooler, regenerator and freezer. The attainment of the highest heat-transfer however, involves new difficulties, since the components mentioned each constitute a resistance to the gas flow from the compression space to the expansion space and back. To overcome this flow-resistance a certain difference in pressure between the two spaces is required, for which additional shaft power has to be supplied, and which results in a reduction of the refrigerating capacity. This "flow loss" is intimately connected with the extent of the heat transfer and with the size (total diameter) of the ducts. It will be clear that in practice a compromise is necessary, aiming at a reasonable heat transfer at acceptable values of the flow loss and the dead space.

---

[3]) H. Hausen, Z. angew. Math. Mech., 9, 173-200, 1929.

[4]) Contrary to the adiabatic loss, however, this loss does impair the refrigerating capacity.

It is not easy to give clean-cut directions for determining the values of the parameters relevant to the refrigerating machine; moreover, the choice is, as always, influenced by the designer's personal preference. We must, therefore, confine ourselves to some general observations.

In practice the machine must be designed to satisfy the demand for a certain refrigerating capacity at a prescribed freezing temperature. The refrigerating capacity, which is the output of cold per second, has been given by formula (13) in I, which reads:

$$q_{\mathrm{E}} = 5.136\,\bar{p}\,V_0 \frac{\delta}{1+\sqrt{1-\delta^2}} \sin\Theta \frac{n}{1000} \text{ watt,} \qquad (6)$$

where

$$\tan\Theta = \frac{w\sin\varphi}{\tau + w\cos\varphi}.$$

In the expression (6) only the variables $\bar{p}$ (average pressure), V_0 (volume of the expansion space) and n (number of r.p.m.) can be chosen without restriction. τ is prescribed by the freezing temperature, whilst δ, φ, and w are more or less fixed for a well-designed refrigerator, viz. $0.3 < \delta < 0.4$, $60^\circ < \varphi < 120^\circ$, and w has the order of magnitude 1.

In view of the fact that the refrigerator should preferably be as small as possible for a given capacity (and hence V_0 should be small), $\bar{p}$ and n have to be selected as high as possible. In raising n one is handicapped by increasing losses (mechanical loss and flow loss) and by criteria concerning the operating life of the machine. In practice, therefore, it is only the value of $\bar{p}$ that can be freely varied. *Increasing the pressure level, is indeed a most effective means of drastically reducing the size of the gas refrigerating machine,* contrary to the evaporation refrigerator, where this cannot be done. The raising of the working pressure is limited by mechanical considerations, such as the required strength of the partition walls and the load applied to the drive.

Still another factor precludes undue raising of the pressure level. According to formula (6) the refrigerating capacity should increase linearly with rising pressure. In practice, however, losses occur which cause the refrigerating capacity to increase less than linearly. The higher the pressure, the greater the relative influence of the loss, until finally the refrigerating capacity will even decrease if the pressure is made still higher (cf. *fig. 4*). It was because of this effect that our experimental machines were initially unable to reach temperatures below —160 °C (the loss increases at lower freezing temperature), a behaviour which baffled us for a long time. We finally came to the conclusion that the interaction between the regenerator and the rest of the machine is responsible for this behaviour. As already mentioned, the average temperature of the regenerator mass varies periodically as a result of the periodic accumulation and discharge of heat. This affects the normal pressure cycle of the machine and results in a smaller refrigerating capacity (as well as decreased shaft power). This effect is governed by the ratio of the thermal capacity of the regenerator mass to that of the gas contained in it; the smaller the value of this ratio, the more is the linearity impaired. The ratio becomes smaller as the denominator increases, which happens if the pressure level in the machine is raised or the freezing temperature lowered: in both cases the quantity of gas in the regenerator is increased. These considerations adequately explain the non-linear behaviour, and calculations of the effect agreed well with the actual measurements. According to this explanation, the effect can be minimized by choosing the highest possible thermal capacity per cm³ for the regenerator mass. This requirement is in addition to that of classical regenerator theory (cf. footnote [3]), according to which the total thermal capacity of the regenerator must exceed a certain prescribed value.

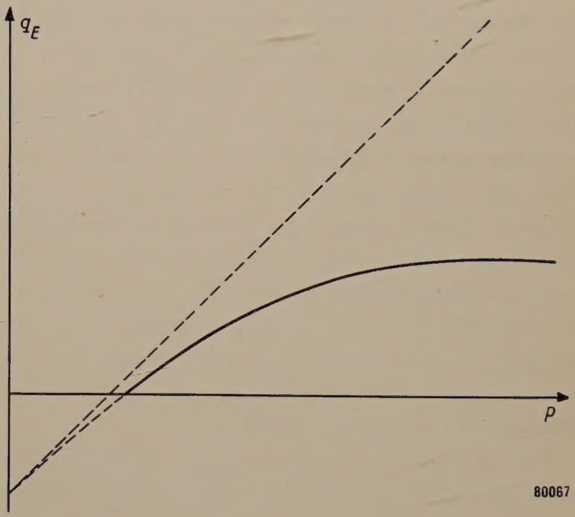

Fig. 4. Variation of the refrigerating capacity q_{E} with the pressure p in the refrigerator. According to the theoretical formula (equation) (13), part I) the dotted straight line would be expected. The measured curve deviates from this straight-line as shown by the full ciurve. Clearly there is a surprising decline of the refrigerating capacity at increasing pressure in the high-pressure range.

It is now convenient to deal with the actual refrigerating machine developed in the Eindhoven laboratories. The way in which the volume variations are effected in this machine, is somewhat different from what has been described in I. This type of machine is termed a "displacer machine"; its working principle is outlined below.

The displacer machine

It has been found that the displacer-type of mechanism, which was used in some of the old hot-air engines, has certain particular advantages for the refrigerator. The principle is illustrated in *fig. 5*. The volume variations are no longer obtained with the aid of two equivalent pistons, but by means of a main piston and an auxiliary piston, which is termed the "displacer". The main piston *1* moves in a cylinder *2* and varies the volume of the entire working space. This working space is divided by the displacer *3*, which like the main piston, has a harmonic motion: there is thus a space *4* between main piston and displacer, and a space *5* above the displacer, both spaces varying harmonically. The displacer motion is such that space *4* is lagging in phase with respect to space *5*, so that space *4* is the compression space and space *5* is the expansion space (cf. I); this is illustrated in the graph in *fig. 6*.

The spaces *4* and *5* are in open communication with one another via the annular heat exchanger surrounding the displacer. The gas pressures above and below the displacer are nearly the same (hence the name "displacer"). Owing to this, there is only a slight leakage of gas from the expansion space so that the accompanying loss of cold is very slight, which is a substantial advantage of the displacer-type machine. In a machine having two normal pistons this loss of cold is considerably greater, due to the far greater pressure differences. Another advantage of the displacer machine is the far smaller mechanical loss, thanks to the small frictional loss of the displacer.

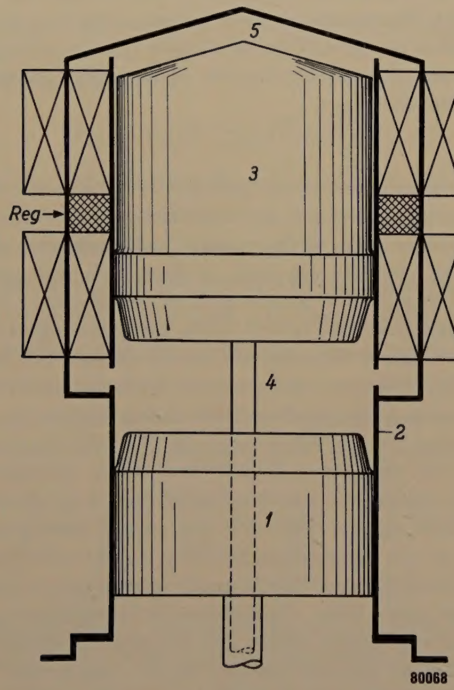

Fig. 5. Principle of the displacer machine. *1* = main piston, moving in cylinder *2*. *3* = displacer, causing a periodic flow of gas back and forth between the spaces *4* and *5*. The gas then flows through the annular heat exchangers surrounding the displacer.

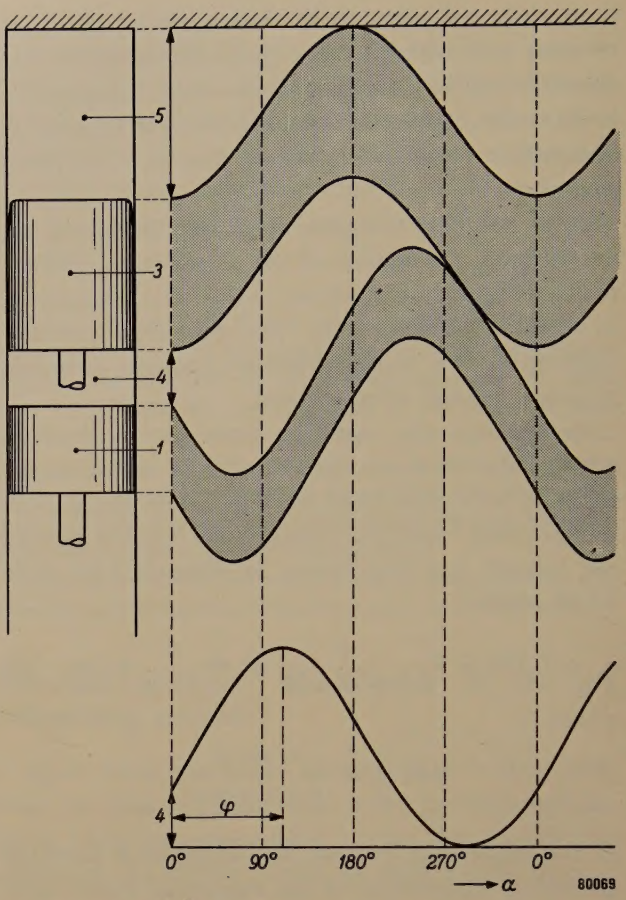

Fig. 6. Variations of the volumes of spaces *4* and *5* of fig. 5 as functions of the shaft angle α. The constant volumes taken up by the displacer body (*3*) and by the body of the main piston (*1*) are shown in grey. The fixed head of the cylinder is shown shaded. In the lower part of the diagram the volume of space between displacer and master piston has been plotted separately, in order to demonstrate its sinusoidal variation and the phase shift with respect to space *5*.

Description of the gas refrigerating machine

The machine is shown in *fig. 7*. The components already mentioned are marked by the same numbers. The main piston is driven, via two parallel connecting rods *6*, by the cranks *7* of the crankshaft *8*. The displacer rod *9* passes through the centre of the main piston to the crankcase, where it is coupled, via the connecting rod *10*, to a third crank *11* of the crankshaft. The angle between the cranks *7* and *11* has been so chosen that the motion of the displacer has the desired phase difference with respect to that of the main piston. The gas flows out of the compression space through the ports *12* to the space containing the cooler, the regenerator and the freezer; the upper end of the freezer communicates with the expansion space.

The displacer consists of a piston body *16* and the "cap" *17*. The piston body carries piston rings and fits in the cylinder liner as a normal piston, and has about the same temperature as the liner, which is surrounded by cooling water. The cap is made of a heat-insulating material and is filled with a loose woolly substance in order to preclude gas circulation within the cap. The cap has a slightly smaller diameter than the piston body, so that it does not touch the cylinder. All these provisions considerably reduce the loss of cold through conduction to the warm parts of the machine.

This construction, the principle of which was applied in the earliest hot-air engines, provides an elegant solution of the problem of how to seal a cold space by means of a moving piston at the ambient temperature, without loss of cold. It is remarkable that the designers of expansion engines for the liquefaction of air have overlooked this solution, which could have saved them many a difficulty.

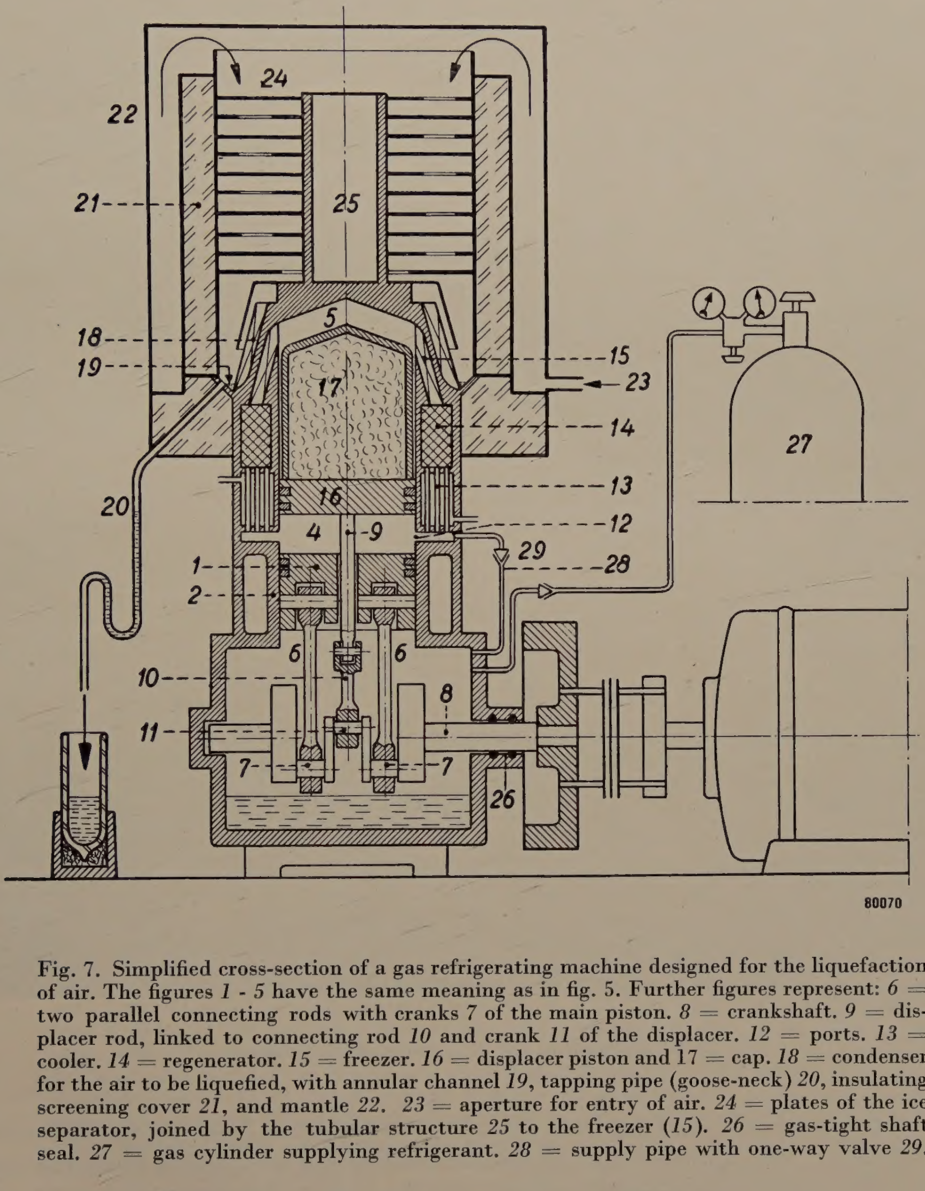

Fig. 7. Simplified cross-section of a gas refrigerating machine designed for the liquefaction of air. The figures *1 - 5* have the same meaning as in fig. 5. Further figures represent: *6* = two parallel connecting rods with cranks *7* of the main piston. *8* = crankshaft. *9* = displacer rod, linked to connecting rod *10* and crank *11* of the displacer. *12* = ports. *13* = cooler. *14* = regenerator. *15* = freezer. *16* = displacer piston and *17* = cap. *18* = condenser for the air to be liquefied, with annular channel *19*, tapping pipe (goose-neck) *20*, insulating screening cover *21*, and mantle *22*. *23* = aperture for entry of air. *24* = plates of the ice separator, joined by the tubular structure *25* to the freezer (*15*). *26* = gas-tight shaft seal. *27* = gas cylinder supplying refrigerant. *28* = supply pipe with one-way valve *29*.

The outside of the freezer forms the "condenser" *18*, against which the air can condense. The liquified air is collected in an annular channel *19* and can be tapped via a pipe *20*. The condenser is surrounded by an insulating screening cover *21* and a mantle *22*. Fresh air can enter through the aperture *23* and flow through holes in the plates *24*, which are thermally connected via the tubular structure *25*, to the freezer. The water vapour and the carbon dioxide

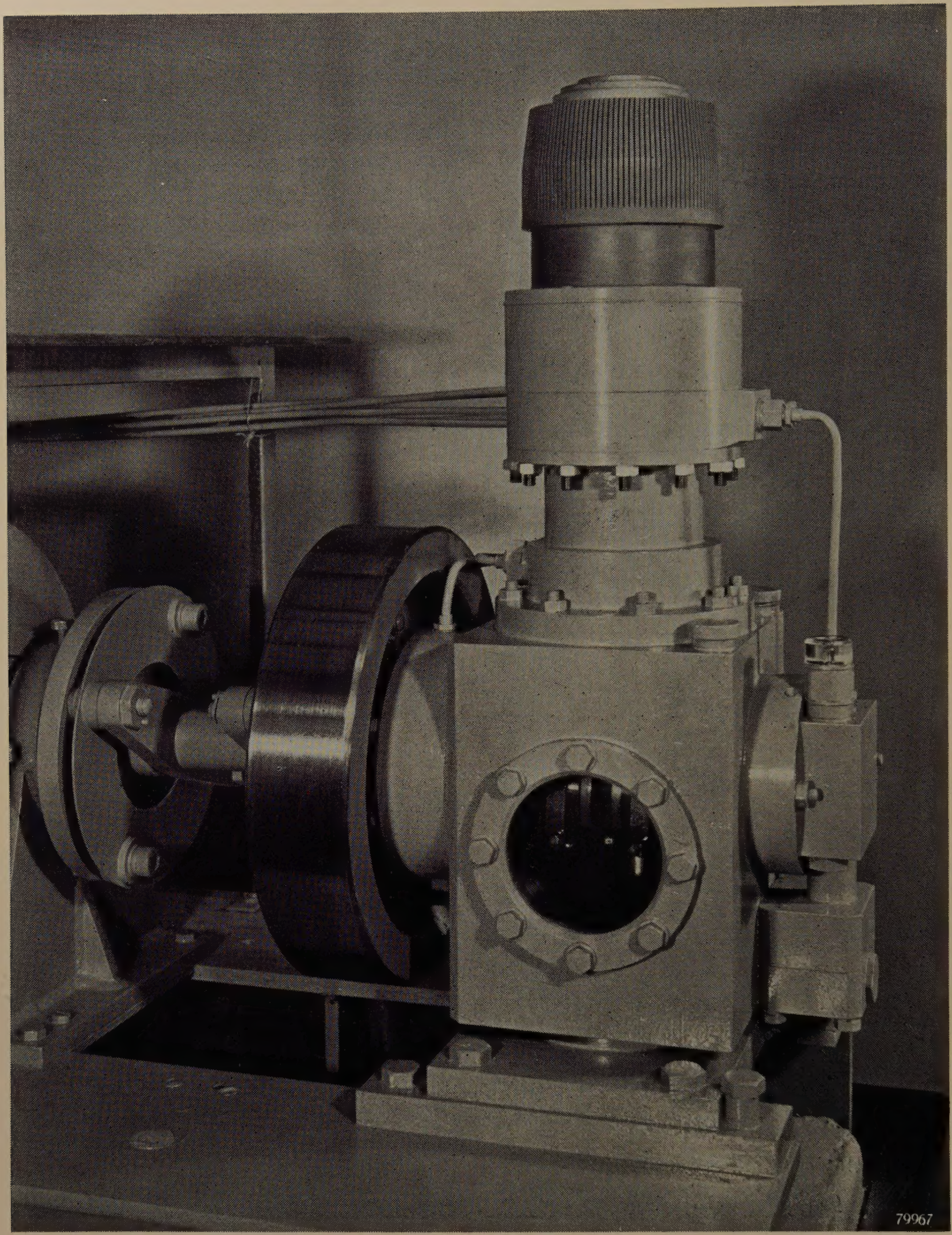

Fig. 8. Photograph of the gas refrigerating machine.

contained in the air will precipitate as a frost on these cold plates (termed the "ice separator"), so that the condenser *18* is not contaminated by ice or solid CO_2.

The complete refrigerator is shown in *fig. 8*. *Fig. 9* is a photograph of the cooler, the regenerator and the cylinder head. We shall now proceed to discuss some of the details of the machine.

Constructional features

The crankcase is closed and contains the gas serving as the refrigerant; the gas pressure is approximately equal to $p_{\min}$ in the working space. The crankshaft is led out via a shaft seal (fig. 7, *26*). The filling gas is supplied from the cylinder *27* to the crankcase; from there, pipe *28* with one-way valve *29* leads to the working space.

Whenever leakage round the main piston (which reduces the pressure level in the working space) causes $p_{\min}$ to drop below the pressure in the crankcase, the gas will flow back to the working space through *28*. In principle the machine is gas-tight; and only if incidental leakage has caused the gas pressure to fall below the necessary level is the machine replenished from the supply cylinder.

The crankcase has to be of comparatively heavy construction to cope with the high gas pressure applied. A pressurized crankcase offers some substantial advantages over a crankcase at atmospheric pressure. With a pressure $p_{\min}$ in the crankcase, the pressure difference exerted on the main piston is far smaller (varying between 0 and $(p_{\max} - p_{\min})$), than in case of operation under atmospheric pressure, when the difference would vary between $p_{\min}$ and $p_{\max}$. The forces acting upon the drive and moving parts are thus smaller and so are the frictional losses. The gas leakage round the piston is likewise less; also the amount of gas thus lost is automatically returned to the working space, which would otherwise not be possible. Finally it provides the means of drastically curbing leakage of gas from the machine since, unlike a piston, a rotating shaft can be provided with a perfectly gas-tight seal.

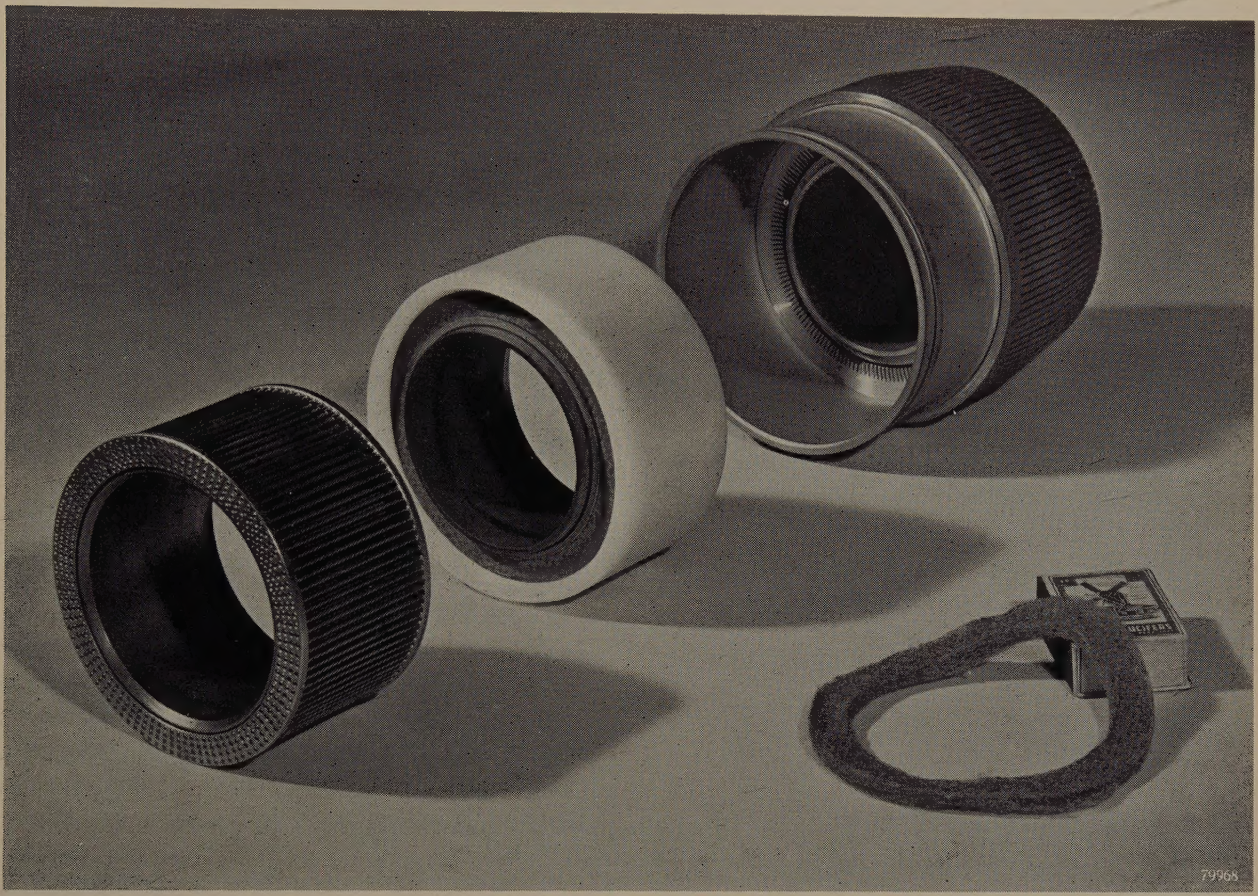

Fig. 9. Left to right: cooler, regenerator and cylinder head (of which the freezer and the condenser form integral parts) of the gas refrigerating machine.

The cooler is built-up of a large number of thin pipes, parallel to the axis of the cylinder. The refrigerant gas flows through these pipes, which are surrounded by the cooling water; this water also cools that part of the cylinder wall along which the displacer moves (see figs. 5 and 7).

The regenerator, like that of the hot-air engine, consists of a mass of extremely fine metal wire. Several rings of this material (one ring is shown on the right) are stacked together and kept in shape by two concentric rings of heat-insulating material (in this case nylon). The outer wall of the machine at the location of the regenerator should also be a poor conductor of heat in the axial direction to avoid “short-circuiting” of the regenerator. It has therefore been made of a steel of great strength but poor thermal conductivity, which, although extremely thin, is capable of withstanding the pressure inside the refrigerator.

The freezer is formed by the massive cylinder head, in which a large number of very fine slots have been cut. The outside of the cylinder head (i.e. the condenser) is also provided with a large number of slots in order to improve the heat exchange with the air to be liquefied. The cylinder head is made of copper to ensure the slightest possible temperature difference between the exterior and interior of the refrigerator.

A particularly tricky problem was the fact that the working space had to be completely free of oil, since this would freeze in the colder parts of the regenerator and clog them up. After extensive research it was found possible to give the piston such a shape that despite ample lubrication of all parts subject to friction, no oil can enter the working space. This subject will be dealt with in a separate article.

The pipe from which the liquid is tapped off forms a goose-neck, thus providing a liquid seal. Non-purified air is, therefore, prevented from entering along this pipe and contaminating the condenser. Liquid air can be tapped off notwithstanding the fact that the gas pressure around the condenser is slightly lower than that of the ambient atmosphere because of the flow resistance between the inlet opening and the condenser; the liquid in pipe *20* simply assumes a level above the highest point of the goose-neck. As a consequence of this, fresh air is, as it were, sucked into the machine at just the rate at which it can be condensed (i.e. in accordance with the refrigerating capacity). *No special means are thus required to supply the condenser with air; the refrigerator itself sucks in the required quantity.* As a result of this, the temperature of the condenser is fixed at the condensation point of atmospheric air, viz. —194 °C. This clearly demonstrates the essential simplicity of the installation, owing to the fact that the air is condensed at atmospheric pressure.

Some data and results

The following list provides some data on the machine:

Cylinder bore	70 mm
Piston stroke	52 mm
Crankshaft speed	1440 r.p.m.
$p_{\max}$	35 kg/cm^2
$p_{\min}$	16 kg/cm^2
$p_{\max}/p_{\min}$	2.2 .

The refrigerant used is hydrogen or helium; air is obviously out of the question in view of the fact that at any excess pressure it would be liquefied above the normal boiling point (at 35 kg/cm^2 air liquefies at —144 °C).

In the laboratory, the following measurements were made when using cooling-water at a temperature of 15 °C:

Yield	with dry air	5.8 kg/h
	with moist air	4.8-5.8 kg/h
Shaft power		5.8 kW
Specific shaft power [5])		1.0 kWh/kg of air
Starting-up period		approx. 13 minutes
Period of continuous operation	dry, CO$_2$-free air	several days
	moist air [6])	20-30 hours

Fig. 10 shows the measurements for higher freezing temperatures; the diagram also shows the figure of merit curve (cf. fig. 2).

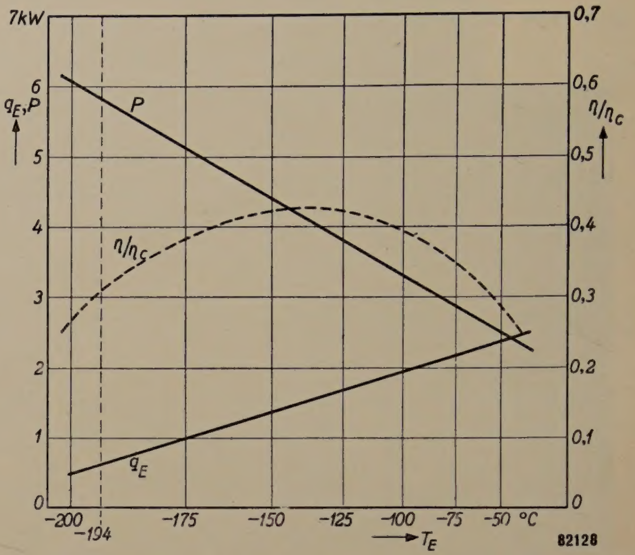

Fig. 10. Measured shaft power P and refrigerating capacity q_E of the gas refrigerating machine plotted as functions of the freezing temperature T_E. The figure of merit η/η_c (cf. fig. 2) derived from this, has also been plotted.

The value of the specific shaft power, which is a measure of the coefficient of performance ("efficiency"), requires some further explanation. The values given in the literature for the specific shaft power of various liquefiers vary within wide limits. With very large installations (producing 100-1000 kg/h), using expansion turbines, a specific shaft power of approximately 0.7 kWh/kg can be obtained; for smaller installations (producing a few kg/h) the figures lie between 1.5 and 3 kWh/kg. We see, therefore, that the efficiency of the gas refrigerating machine, in spite of its small capacity, approaches very nearly that of the large installations.

The scope of this article does not allow an analysis of the cause of this relatively high efficiency; this would require a comparison of the gas refrigeration cycle with other systems, which are quite different. It may suffice here to mention two points in this connection. First of all the pressure ratio (approx. 2.2) is small, so that the adiabatic losses (which play a part in the compressors of the other systems) are small. In the second place there is the circumstance that the power released upon expansion, is recovered by extremely simple and therefore efficient means, viz. by the gas pressure acting upon the piston.

The efficiency of the process, moreover, can be improved a great deal. No less than half the cold produced by the machine is spent in cooling the air; the remainder is used for condensation. By means of a second refrigerator the air may be pre-cooled to an intermediate temperature, so that part of the necessary cold is obtained with a higher efficiency: consequently the overall efficiency is improved. It has been calculated that by means of an intermediate stage of this kind the specific shaft power can be reduced below 0.8 kWh/kg.

---

[5]) For liquefiers, kWh/kg is a familiar measure of the "efficiency" of the installation; in order to avoid ambiguity concerning the word "efficiency", however, we have introduced the designation "specific shaft power" for this quantity (which may be read as kW per kg air/hour). It applies to the liquefaction of dry air.

[6]) The period of continuous operation depends on the volume of the ice separator. Whenever this is clogged up, it has to be defrosted, which takes, inclusive of the new starting-up period, approximately 1 hour.

The gas refrigerating machine compares favourably with the conventional types not only in efficiency but also by its simplicity of operation and by the fact that it is not subject to contamination by dirt and dust (no expansion valves, etc.). An additional advantage is that the liquid air is completely free of oil, owing to the fact that the air need not be compressed.

Moreover, the refrigerating capacity can be varied both by changing the speed of rotation and by varying the gas pressure in the working space: hence a very simple *control* is achieved.

We shall conclude this article by giving a rough survey of the possible applications of the gas refrigerating machine. It will already be clear that the machine can be of great use in laboratories and factories for the production of liquid air. For use in laboratories particularly it will be of great value that other gases, such as nitrogen, argon, oxygen or methane can also be conveniently liquefied by this refrigerator. In this way liquid baths with a well defined boiling point can be made readily available. Preliminary tests have revealed that in certain cases the machine can be successfully used for gas separation, e.g. the fractionation of air. Finally, it can be employed as a pre-cooler for hydrogen that is to be liquefied on a small scale with the conventional type Linde-liquefier *).

The optimum working range of the machine, as previously mentioned, lies between —80 °C and —200 °C, where it can serve as a source of cold for any desired purpose. The machine has a good efficiency (cf. fig. 10) and is considerably less complicated than the cascade machine used up to now in this field. A further great advantage is that any temperature in this range is obtained with the one machine in a single stage. The simplicity and convenience of this refrigerating machine will undoubtedly act as a stimulus in low temperature research.

---

*) See this issue, p. 116. - Ed.

Summary. In its practical form the gas refrigerating machine, is subject to certain losses. Some of these losses increase the shaft power (mechanical loss and adiabatic loss), others cause a reduction of the refrigerating power (insulation loss and regeneration loss). The former group of losses define the upper limit and the latter group the lower limit of the useful temperature range of the gas refrigerating machine (—80 °C to —200 °C). After a brief consideration of these and other losses and their quantitative significance, this article deals with the factors that influence the design of such a refrigerator. Of considerable practical importance is the fact that the volume of a refrigerating machine of given refrigerating capacity can be drastically reduced by using a high pressure level. A description is given of a small machine in which the pressure varies between 16 and 35 kg/cm^2, at a crankshaft speed of 1440 r.p.m. This machine is built on the displacer principle, which was applied in some of the early hot-air engines, and is used for liquefying air. Ownig to the fact that the air does not require a preliminary compression, this liquefier is of very simple design and is easily operated. It has an output of approx. 5.5 kg liquid air per hour and the "specific shaft power" amounts to 1.0 kWh per kg of liquid air — a value which is extremely low for such a small and simple machine, and which may be even further reduced without undue difficulty. In conclusion the article deals with the properties and further potential applications of the gas refrigerating machine.

LIQUEFACTION OF HYDROGEN

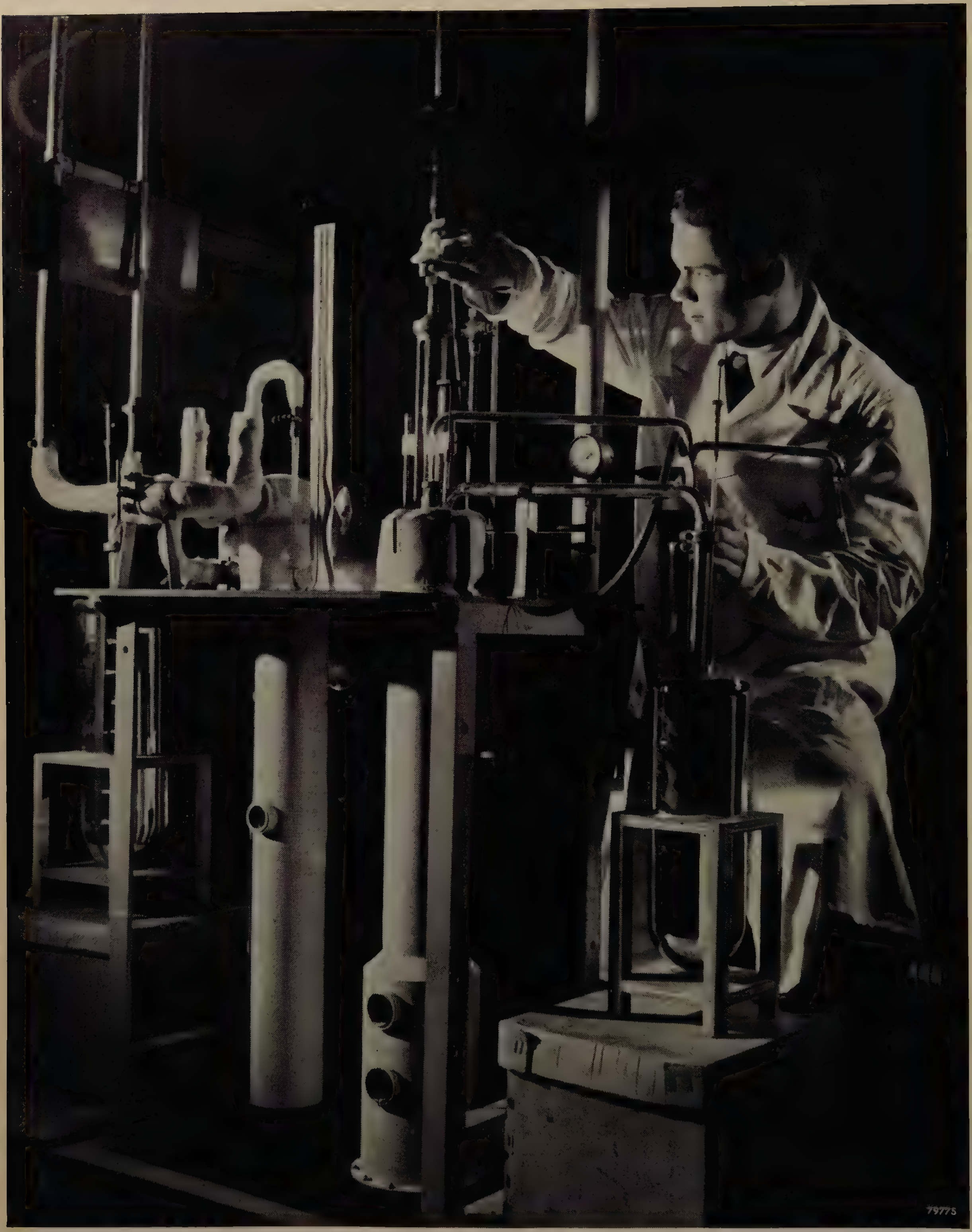

Photo Walter Nürnberg

The investigation of the solid state has made remarkable advances in the last two decades. This work has been particularly fruitful in electronic and electrotechnological applications (ferromagnetic materials, semiconductors, dielectrics, luminescent substances, etc.).

In these investigations it is sometimes important to work at very low temperatures, e.g. when it is required to minimize thermal agitation of atoms and molecules, which may otherwise complicate or mask a phenomenon. In this connection, a simple hydrogen liquefier using a liquid nitrogen pre-cooler is installed in the Philips Research Laboratories. Liquid hydrogen has a boiling point of 20.4 °K at standard atmospheric pressure. The white tubes shown in the photograph contain the equipment for the cleaning and pre-cooling of the gas and also the liquefier proper. The operator is in the process of syphoning some liquid hydrogen into a Dewar flask.

AN ELECTRONIC D.C. MILLIVOLTMETER

by A. L. BIERMASZ and A. J. MICHELS.

621.317.321.027.21

Electronic meters for measuring alternating current, comprising an amplifier, a rectifier and a moving-coil instrument, are sufficiently well known. When such meters are preceded by D.C.-A.C. voltage convertors, they can also be used for the measurement of D.C. voltages. In this way a meter of very high input resistance is obtained and the use of D.C. amplifiers is avoided. A meter designed along these lines is described in the following article. The objection to many electronic meters — that they can be used only where A.C. mains are available — is eliminated by using dry batteries for the supply voltages.

This article describes an electronic D.C. voltmeter suitable for a wide variety of measuring ranges between 1 mV and 300 V. It can be used in place of ordinary moving-coil voltmeters and mirror galvanometers. Compared with the latter it has the advantages of much greater robustness, better ability to withstand overloads, and smaller inertia. An advantage of this instrument compared with conventional voltmeters is the very much higher input resistance, which greatly widens the useful scope. The input resistance is of the order of 1 MΩ in the lower measuring ranges and 100 MΩ in the higher values. For a full-scale deflection of say 1 mV, the current taken is 1.5×10^{-9} A, which corresponds to an input power of not more than 1.5×10^{12} W. In contrast with most conventional electronic voltmeters the present instrument is operated from dry batteries, so that its usefulness is not limited to places where A. C. mains are available; one application in particular where this is a great advantage is in the use of strain gauges out of doors [1]). Another useful feature of this battery-operated instrument is that measurements can be taken between two points which are both at a high potential with respect to earth (with mains-operated meters the voltage is limited by the breakdown field strength of the insulation between the windings of the power transformer); it is, of course, necessary to insulate the meter itself.

When faced with the problem of constructing an electronic D.C. meter the designer will probably first turn his thoughts to a combination of D.C. amplifier and moving-coil instrument. With an ordinary valve in the input stage a high input impedance is then obtained (10^9 ohms). In view of the required sensitivity (full deflection on 1 mV) the unavoidable drift is then fairly great, viz. about 0.3 mV per hour [2]). Moreover, D.C. amplifiers necessitate carefully stabilized supply voltages; in the laboratory this is no obstacle, but in transportable, battery-operated equipment it would certainly be a problem.

A better method consists in converting the D.C. voltage to be measured into an A.C. voltage, and to measure this with an ordinary electronic A.C. meter consisting of an A.C. voltage amplifier, a rectifier and a moving-coil instrument.

There is a choice of two methods of converting the D.C. voltage into an A.C. voltage, viz. the vibrating capacitor or the vibrating contact.

The first of these has already been described on various occasions in this Review [3])[4]), the principle being as follows. The D.C. voltage to be measured is applied to the vibrating capacitor with a high resistance is series with it. The capacitor itself consist of two plates, one fixed and one moving, with air dielectric. An moving coil loudspeaker unit fed from a valve oscillator vibrates the moving plate, thus producing a periodic variation in the capacitance. In the same way as in capacitive microphones, an alternating voltage is thus produced across the capacitor, the amplitude of which is proportional to the applied D.C. voltage.

This method, too, has the advantage of a very high input resistance (about 10^{10} ohms). It will give good results provided that the voltage to be measured is not too small. If this is of the order of millivolts, however — and our meter is to be suitable for measuring fractions of a millivolt — difficulties are experienced owing to the fact that the vibrating capacitor produces an appreciable A.C. voltage even in the absence of any D.C. voltage. This effect can be attributed to the small differences in the work function of the materials of which the capacitor plates are made [5]). By making the plates of the same metal, which must be quite pure, we can reduce this effect to a few millivolts, but this is still not low enough for our purpose and, moreover, the voltage is likely to rise owing to the entry of dust and damp into the components; an instrument used in the open air would be more than usually exposed to these.

---

[1]) A. L. Biermasz and H. Hoekstra, Philips tech. Rev. **11**, 23-31, 1949/50.

[2]) A very much higher input impedance (10^{14} Ω) can be obtained with the electrometer triode (H. van Suchtelen, Philips tech. Rev. **5**, 54-59, 1940), but the drift in this instrument is appreciably greater.

[3]) C. Dorsman, A *p*H meter with a very high input resistance, Philips tech. Rev. **7**, 24-32, 1942.

[4]) J. van Hengel and W. J. Oosterkamp, A direct-reading dynamic electrometer, Philips tech. Rev. **10**, 338-346, 1948/49.

Preference has therefore been given to the vibrating-contact method. The contact periodically short-circuits the input of the A.C. amplifier and thus produces a square-wave voltage, alternating between the value to be measured and zero.

The output current from the amplifier has to be measured with a moving-coil meter and must accordingly be rectified, this latter being achieved by means of a second vibrating contact which opens and closes exactly in phase or in antiphase with the first-mentioned contact.

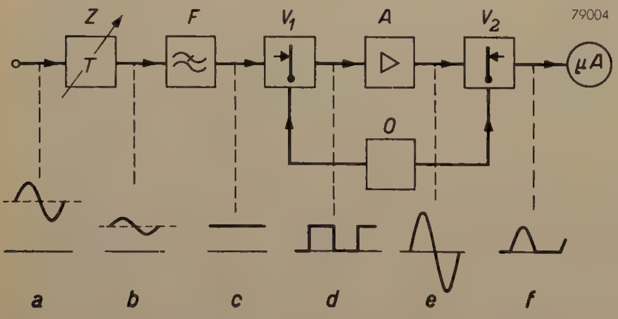

Fig. 1. Block diagram of the D.C. voltmeter GM 6010. *Z* variable attenuator (T-network). *F* low -pass filter. V_1 vibrator to convert the D.C. voltage to a square-wave voltage. *A* A.C. voltage amplifier. V_2 vibrator to rectify the output current of the amplifier. *μA* microammeter. *0* oscillator for driving the vibrator.

a represents the D.C. voltage to be measured, including ripple. *b* attenuator output voltage. *c* voltage at output of filter. *d* square-wave voltage. *e* amplifier output voltage. *f* half-wave rectified current passing through the meter.

The instrument further includes a variable attenuator for adjustment of the meter to the desired measuring range, and a filter for suppressing any A.C. voltage that may be superimposed on the D.C. voltage (see block diagram, *fig. 1*).

The complete unit [6]), the Type No. of which is GM 6010, is depicted in *fig. 2*; *fig. 3a* shows the battery compartment and fig. 3*b* the chassis.

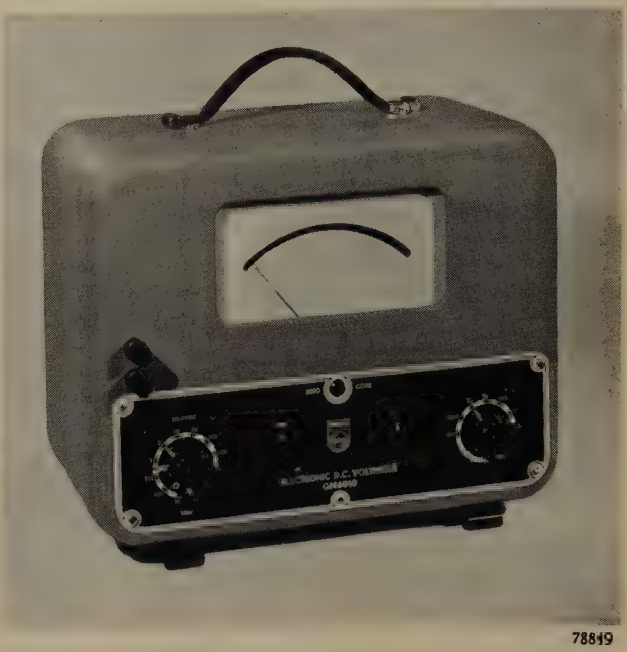

Fig. 2. The millivoltmeter GM 6010. Left to right, attenuator control, zero adjustment (compensating current), gain correction control, and multi-position switch for zero correction, measurement of the battery voltages, calibration, and reversal of polarity.

The vibrator

The contacts

The functions of the two vibrators illustrated in fig. 1 are combined in a single flat spring which alternately makes contact with contact screws mounted on each side of it (*fig. 4*).

In order to avoid errors in measurement, the making and breaking must take place without any chattering, and the time taken by the spring to travel from the one contact to the other must be short (about 2%) compared with the complete period. To ensure that no chattering will take place, the velocity at which the spring strikes the contact points must be low [7]). To ensure this, the contact screws are mounted near the clamped end of the spring where the amplitude of vibration is small and of a very definite value (about 10 μ); the amplitude of the free end of the spring is then about 0.5 mm. This arrangement also achieves a time of travel short compared to the time the contacts are closed.

---

[5]) See p. 28 of article [3]).

[6]) The design of this meter was commenced by J. M. L. Janssen, who has since left the service of the Company.

[7]) Cf. J. A. Haringx, Vibration of contact springs, Philips tech. Rev. 7, 155-158, 1942.

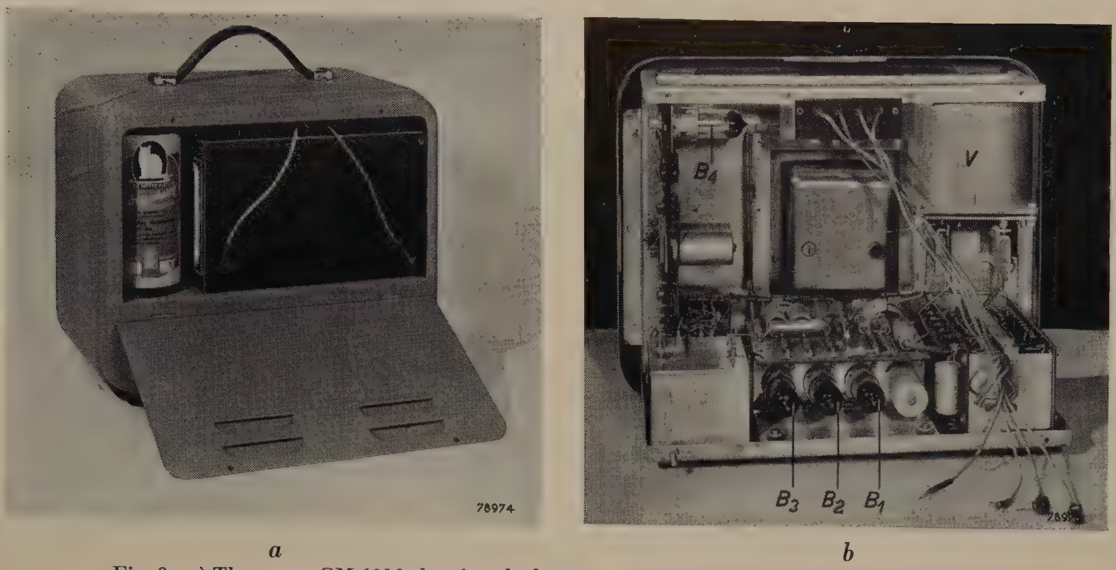

a b

Fig. 3. *a*) The meter GM 6010 showing the battery compartment. *b*) the chassis; B_1, B_2 and B_3 are the amplifier valves; B_4 is the oscillator valve. *V* is the vibrator.

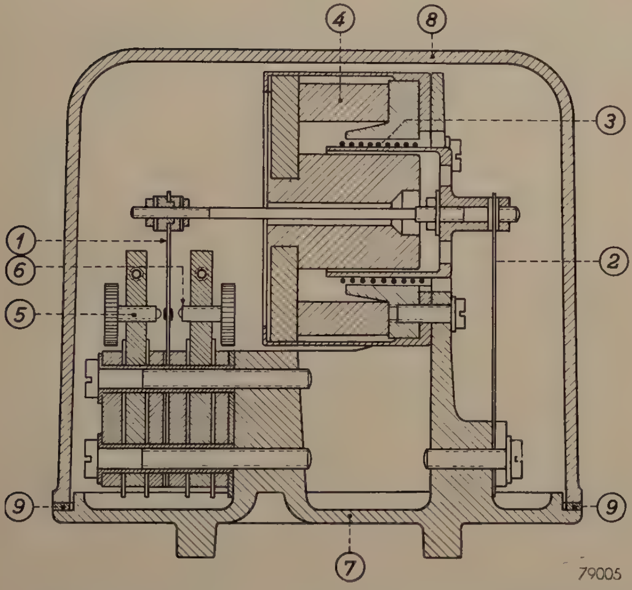

Fig. 4. Cross section of the vibrator. *1* and *2* are flat springs clamped at one end and maintained in vibration by an electrodynamic driving system comprising coil *3* and permanent magnet *4*. The spring *1* makes contact alternately with screws *5* and *6*. *7* base plate; *8* housing; *9* rubber gasket.

Whether contact is made and broken without chattering and whether the time of travel is sufficiently short, can be checked by means of the circuit shown in *fig. 5a* in conjunction with a cathode-ray oscilloscope, which should then produce a trace such as that shown in fig. 5*b*.

In the design of the vibrator the following possible sources of measuring errors were taken into account:

1) thermo-e.m.fs due to local heating at the contact points [8]).
2) contact potentials set up by differences in the chemical composition of the metals used for the vibrating contacts.
3) electrical double layers formed by the entry of dust and moisture.

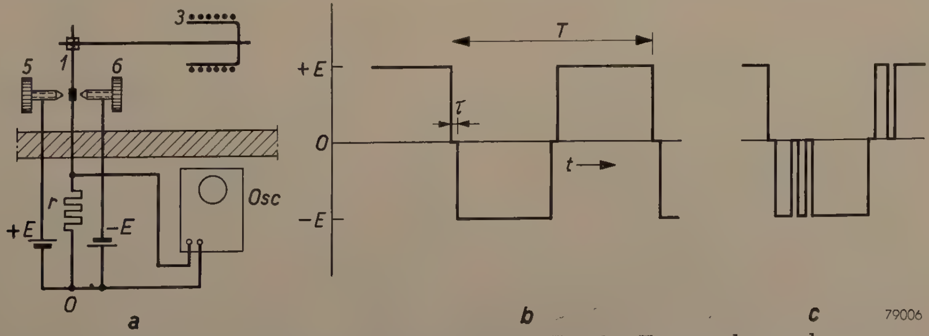

a b c

Fig. 5. *a*) Circuit for testing the vibrator; voltages $+E$ and $-E$ occur alternately across the resistor *r*. The oscilloscope *Osc* should show the image given in (*b*), without interfering pulses as in (*c*) and with a change-over time τ equal to roughly 2% of the period *T*. Other references as in fig. 4.

---

[8]) The faces of the contacts in unused vibrators are relatively soft. Vibrators are "run-in" for some time in the factory: during this process the microscopically small projections from the faces are melted off, which suggests increases in temperature which are quite considerable though of short duration. This running-in makes the contact faces smoother and harder, so that no further changes in shape take place.

These sources of error are minimized by taking the following steps: the contact pressure is made small (i.e. very flexible contact spring), gold is used as contact material (this is better than platinum or rhodium, for example), and the vibrator is made as airtight as possible.

In this way it has been found possible to reduce the residual voltage arising from the causes listed above to 20 or 30 μV, i.e. to a value that is some thousandths of that occurring with a vibrating capacitor.

The meter is provided with an adjustment for eliminating the small deflection resulting from this residual voltage (2 or 3 scale divisions); this is done by passing a small variable compensating current through the meter in the opposite direction.

Maintaining the vibration

The simplest system whereby the vibrator can be kept in motion is that of the ordinary trembler bell. All that is needed is a solenoid with an additional contact on the vibrating armature, the whole being fed from the source of filament current. This system does not give satisfactory results however, as the armature spring readily assumes modes of vibration other than the fundamental and therefore cannot be made to work without chattering.

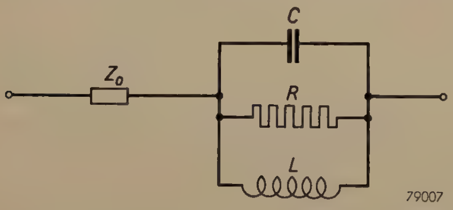

Fig. 6. Equivalent circuit of the vibrating coil. Z_0 = impedance of coil at rest.

We have accordingly adopted an electrodynamic drive of the kind shown in fig. 4. Alternating current for the driving coil is supplied by a Hartley oscillator using a DAF 41 valve. The oscillatory element is the coil itself, the equivalent circuit of which is depicted in *fig. 6*. The total impedance Z of this element should be high at the resonance point, in order to satisfy the condition of oscillation even when the mutual conductance S of the oscillator valve is low; that is: SZ = constant.

The parameters C, R and L in this circuit can be derived from the mechanical data. Let us denote the moving mass by m, the spring constant by c, the damping factor by k, the velocity by v and the angular frequency by ω. The force acting on the moving system in the stationary condition is then:

$$F = \left(j\omega m + k + \frac{1}{j\omega c}\right) v \quad . \; . \; . \; . \; . \; . \quad (1)$$

If we further denote the terminal voltage of the coil by e, the induced electromotive force by e_i, the impedance of the coil at rest by Z_0 and the current by i, then:

$$e = iZ_0 - e_i \, . \quad . \; . \; . \; . \; . \; . \; . \; . \quad (2)$$

Also:

$$F = ai \quad . \; . \; . \; . \; . \; . \; . \; . \; . \; . \; . \quad (3)$$

and:

$$e_i = -av \, , \quad . \; . \; . \; . \; . \; . \; . \; . \; . \; . \quad (4)$$

where $a = Bl$, B being the magnetic induction in the air-gap, and l the length of wire in the coil.

Elimination of F, v and e_i from (1), (2), (3) and (4) gives the impedance Z of the coil:

$$Z = \frac{e}{i} = Z_0 + \frac{1}{j\omega\frac{m}{a^2} + \frac{k}{a^2} + \frac{1}{j\omega c a^2}} \, .$$

From this and from fig. 6 it follows that $C = m/a^2$, $R = a^2/k$ and $L = ca^2$. At resonance, $\omega m/a^2 = 1/\omega \, ca^2$, so that the resonance frequency is determined by mc, and Z becomes $Z_0 + a^2/k$, where Z_0 is approximately the D.C. resistance of the coil. For easy oscillation a^2/k should be high, i.e. a high (strong magnetic field, many turns), and k small (weak damping).

For our purpose the self-inductance L in the equivalent circuit is 0.25 H and the capacitance C is 20 μF, which gives a resonance frequency of about 70 c/s. At this low frequency the impedance of the coil at rest, Z_0, is almost that of a resistance of 800 ohms. The total impedance of the coil vibrating at its own natural frequency is roughly 7000 ohms, so that oscillation will occur even when the mutual conductance of the valve is low. This high impedance was attained by adopting various measures to reduce the damping; the air damping has been kept low by using a streamlined coil former with perforations. Owing to the flexible suspension, moreover, there is very little loss through a transfer of energy to the framework. The input power of the coil is only a few milliwatts.

The amplifier

A three-stage amplifier is used, with DAF 41 valves in the first and second stages and, in view of the desired linearity, a DL 41 [9]) as output valve (*fig. 7*).

The anode circuit of the output valve includes a transformer whose core is provided with an air-gap to avoid D.C. saturation, which would affect the linearity of the scale. By means of a parallel capacitance, the primary side of the transformer is tuned roughly to the frequency of the vibrator, so that, although the input voltage is of square wave-form, the output voltage is practically sinusoidal.

This parallel capacitance affects the phase of the output voltage. To ensure effective rectification, it is of such a value that the current is zero during the time that the vibrator passes from one contact to the other.

---

[9]) The DL 41 valve is discussed in Philips tech. Rev. **10**, 346-351, 1948/49.

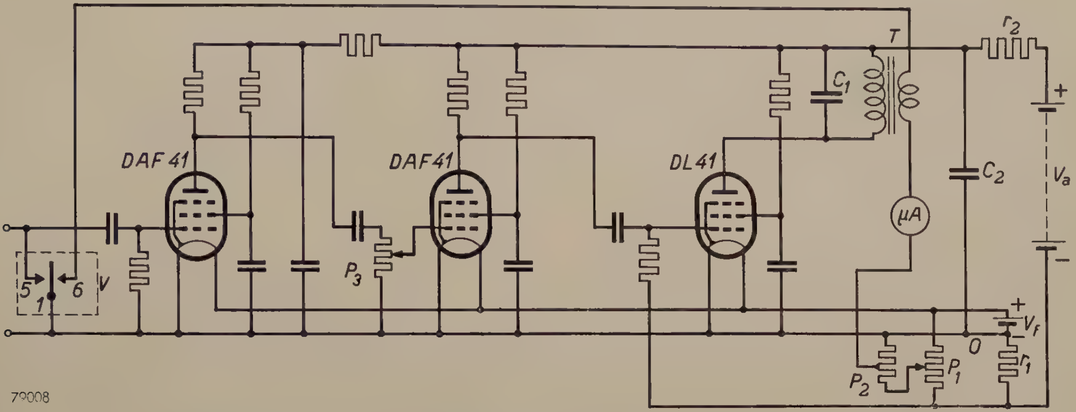

Fig. 7. Simplified schematic diagram of the amplifier and vibrator. *V* vibrator, with spring *1*, shorting contact *5* and rectifying contact *6*. By means of the capacitor C_1, the output transformer *T* is tuned roughly to the frequency of the vibrator (approx. 70 c/s). V_a H.T. voltage (90 V nominal). V_f L.T. voltage (1.4 V nom.) The resistor r_1, through which the anode and screen currents pass, provides bias for the output valve DL 41 and also makes available at the slider of the potentiometer P_1 a positive or negative voltage with respect to the point *O*. By means of P_1 (through the fixed potential divider P_2) a current is passed through the µammeter which is just sufficient to compensate the deflection due to residual voltage. The gain is corrected by means of potentiometer P_3. A 3900 ohm resistor r_2 is connected in series with the H.T. battery to reduce the effect of variations in the internal resistance of the battery. C_2 is a decoupling capacitor.

A moving-coil meter is connected to the secondary side of the transformer, in series with the vibrator, and the current passing through it is therefore half-wave rectified. The advantage of this is that the instrument thus also indicates the polarity of the voltage to be measured; when the polarity is reversed, the other half-cycle of the output current is passed and the meter needle deflects in the other direction. A switch is provided to permit this reversal of polarity.

Other components

The attenuator

This comprises three groups of resistors R_1, R_2 and R_3, arranged as a T-network (*fig. 8*), and a switch controlling them gives a choice of 12 ranges, with sensitivities of 300 V, 100 V, 30 V, ..., 3 mV, 1 mV, full scale deflection. The input resistance is highest (100 MΩ) in those positions in which 1 V or more is required for maximum deflection, and lowest (0.6 MΩ) in the most sensitive position of the switch. The maximum error in the attenuator is 2%.

The filter

The filter follows immediately after the attenuator (fig. 8). The object of the filter is to suppress any A.C. voltage (ripple) which might be superimposed on the D.C. voltage and which would otherwise introduce errors in measurement. The filter consists of resistors and capacitors and is designed to give an attenuation of 500 × for 50 c/s voltages. This means that even a ripple voltage equal to 10 times the D.C. voltage to be measured has little or no effect on the result (provided that the ripple is not greater than 5 V; if this happens, the A.C. voltage arriving at the input of the amplifier via stray capacitances would overload the amplifier).

Early on during the design, the capacitors in the filter presented difficulties. These will now be mentioned.

Dielectric after-effects and frictional electricity

In the original design, standard capacitors with paper dielectric were used in the filter. Now, when the attenuator is set in advance to the required measuring range, a potential of not more than 1 mV occurs across the capacitors. With incorrect handling,

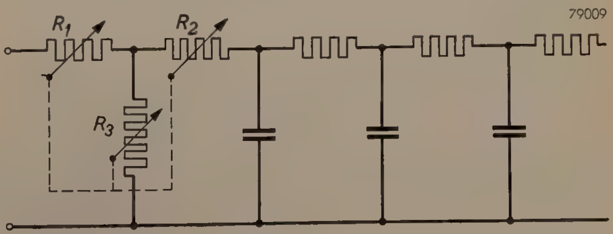

Fig. 8. Attenuator and filter. R_1, R_2 and R_3 are three groups of resistors in a T-network, operated by a single 12-position switch.

however, for example when a 100 V potential is to be measured and the instrument is set for maximum 1 mV, the voltage on the capacitors can be very much higher. The instrument is able to withstand this (because the gain drops considerably on overloads), but the real difficulty was found to be that the discharge of the capacitors takes place very slowly, necessitating an hour's wait before the instrument is again ready for use.

This can be demonstrated by the following experiment. A paper capacitor, of capacitance $C = 0.22$ μF, is charged up to 100 V and is then discharged through a resistor $R = 1.68$ MΩ. At first the voltage will drop in accordance with the anticipated exponential curve with time constant $RC = 0.37$ sec, until a value of about 1 mV is reached. The further voltage drop, which is shown plotted in *fig. 9*, takes place much more slowly: as an approximation, exponentially with a time constant of 165 sec, i.e. roughly 500 RC. It takes about an hour for the voltage to drop to 10 μV (= one division of the scale of the GM 6010). Short-circuiting of the capacitor does not help matters, because as soon as the short is removed, roughly the same voltage occurs again (see A and B, fig. 9).

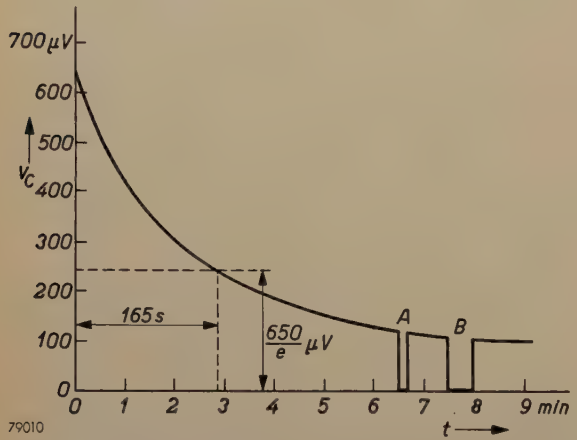

Fig. 9. Dielectric after-effect in a paper capacitor charged to 100 V and discharged through a resistor (time constant $RC = 0.37$ sec). The figure shows the drop in the capacitor voltage from the moment it reaches 650 μV. v_C then diminishes much more slowly than before, more or less exponentially, with a time constant of about 165 sec. Even when the capacitor is short-circuited for different lengths of time (at A and B), the voltage v_C returns to roughly the same value after the short is removed.

This is due to a kind of after-effect; ions are produced in the dielectric which can disappear only slowly. Some materials exhibit this property to a much smaller extent than others; in polystyrene, for example, the effect is very slight indeed and persists for only about 1/50 the time as in paper. For this reason filter capacitors with polystyrene dielectric are used in the GM 6010.

As the insulating material used for the terminal blocks would also be likely to exhibit this effect, polystyrene is used for this purpose as well.

Another source of interference is to be found in frictional electricity generated on the insulating material on the connecting leads, particularly if this is of plastic. Static charges may be set up by friction, flexion or vibration, and these will produce a deflection. Because of this, rubber-covered flex, or, better still, bare leads, if necessary supported by ceramic insulators, are used.

Calibration

For preference, electronic meters should be equipped with means for self-calibration. This applies all the more when the instrument is operated from dry batteries, whose voltage may vary considerably, and when the amplifier, as in the GM 6010, does not use negative feed-back.

In the first place the supply voltages of the instrument are checked to see that they are within the appropriate limits. This is done using the moving coil meter which, with the calibration control set to certain positions, functions as an ordinary voltmeter. The H.T. battery should give a reading between 95 and 75 V, and the filament cell between 1.55 and 1.05 V.

Calibration is effected as follows. A potential divider of fixed resistors delivers a certain fraction ($1/A$) of the L.T. voltage V_f. With the calibration control rotated one stage, this voltage V_f/A is applied to the input of the vibrator, the gain being then so adjusted by means of the gain control (potentiometer P_3, fig. 7) that the meter indicates V_f, i.e. the same deflection as with direct measurement of the L.T. voltage. It is then known that the gain is equal to the fixed value A on which the scale calibration is based.

Summary Description of an electronic D.C. millivoltmeter (type GM 6010), in which the D.C. voltage to be measured is converted by a vibrator into a square-wave voltage which is subsequently amplified by an A.C. amplifier. A second contact on the vibrator rectifies the output current from the amplifier, and this rectified current is passed through a moving-coil meter. The vibrator is driven by an electrodynamic system in which the coil constitutes part of a valve oscillator. The amplifier and oscillator are operated from dry batteries, and the use of the instrument is therefore not limited to places where A.C. mains are available. As the meter is independent of the mains, voltages can be measured between points which are both at a high potential with respect to earth. The vibrator circuit is preceded by a variable attenuator and a filter; the former has 12 positions corresponding to ranges of 300 V, 100 V, 30 V, ..., 3 mV, 1 mV. The input resistance lies between 100 MΩ for ranges of 1 V and upwards and 0.6 MΩ for 1 mV; the filter suppresses A.C. voltages that may be superimposed on the D.C. voltage to be measured. Polystyrene is used for the dielectric of the filter capacitors as well as for the terminal blocks, as this material shows very little electrical after-effect. The instrument is provided with means for self-calibration.

THE "NORELCO" X-RAY DIFFRACTOMETER

by W. PARRISH [*], E. A. HAMACHER † [*] and K. LOWITZSCH [*].

539.262:548.733:
621.387.424

The X-ray spectrometer, described in this Review a number of years ago, has been completely re-designed. The new instrument, which has now been commercially available for some years, will be the subject of this and a following article. The present description is ~~not~~ intended for the instruction of potential users (these are served more fully by special publications of the Company): its main purpose is to reveal the technical basis and implications of the new design.

Introduction

The application of X-ray diffraction analysis as a tool for technical and scientific investigations has gained a firm footing in an ever-increasing number of industrial and university laboratories. The last decade has witnessed the successful introduction into this field of a new method, the direct measurement and recording of line intensities in X-ray diffraction patterns by means of a Geiger counter tube. An instrument based on this principle and known as the "Norelco" Geiger counter X-ray spectrometer was designed and marketed by the North American Philips Company in 1945, and described in this Review about six years ago [1]. *Fig. 1* offers a schematic picture of this instrument; the caption recapitulates some details concerning the forming of the X-ray diffraction pattern and the focusing method.

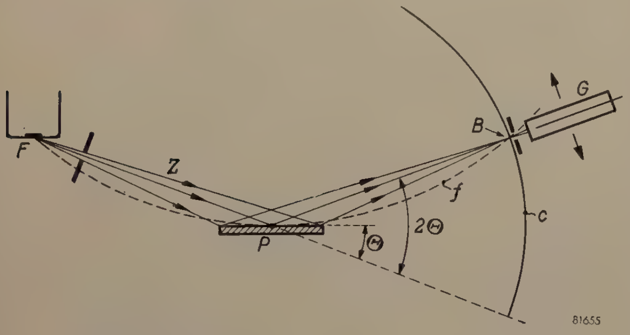

Fig. 1. Focusing arrangement of the Geiger counter X-ray diffraction instrument. A divergent X-ray beam Z coming from the focus F irradiates the surface of a flat specimen positioned at P. All the rays diffracted at Bragg angle Θ by suitably oriented crystallites on the specimen surface converge approximately to a single line, at B. Here the receiving slit of a Geiger counter tube G is placed. The counter tube is moved along the goniometer circle c about the axis P, in order to scan angles 2Θ; the flat specimen is rotated about the same axis at half the angular speed, thus always remaining tangential to the "focusing circle" f through F, P, B (Bragg focusing). (The "focusing" effected is, of course, not true focusing in the optical sense.)

This article describes a completely re-designed version of the spectrometer, whose performance and facilities represent a great advance on those of the first instrument. The new instrument, which from now on will be termed an X-ray *diffractometer* [2], is pictured in *fig. 2*. It comprises three parts, which may be purchased separately and each of which can be used in conjunction with other equipment if desired: a basic diffraction unit (X-ray tube with high voltage generator and controls), a Geiger counter goniometer, and an electronic circuit panel with automatic recorder. The Geiger counter goniometer is shown separately in *fig. 3*.

Although this and a subsequent article will give a self-contained description of the diffractometer, it will be based on a comparison with the former instrument, as this should enable the reader more readily to grasp the significance of a number of details of the design.

Features of the diffractometer

The old and the new instrument alike offer the features characteristic of the method, viz., the instantaneous indication and recording of line intensities and a very considerable saving of time in cases where only part of the diffraction pattern need

---

[*] Philips Laboratories, Irvington-on-Hudson, N.Y., U.S.A. We regret to record the death of Mr. Hamacher on March 25, 1954.

[1] J. Bleeksma, G. Kloos and H. J. di Giovanni, X-ray spectrometer with Geiger counter for measuring powder diffraction patterns, Philips tech. Rev. **10**, 1-12, 1948.

[2] The instrument has been manufactured and marketed for some time by North American Philips Company, Inc., New York, U.S.A., again under the name of X-ray spectrometer. It has now been agreed to reserve the name X-ray spectrograph or spectrometer for the proper classical use in the measurement of X-ray spectra (and for a modified form of the X-ray diffractometer applied to X-ray fluorescence analysis).
Features of the instrument have been previously described by W. Parrish and E. A. Hamacher at A.S.X.R.E.D. meetings 1947-1949, in Science **110**, 368-371, 1949 and in Trans. Instr. Meas. Conf. Stockholm 1952, p. 95.
A similar X-ray diffractometer is now in production in the Philips Works at Eindhoven; the electronic circuit of the latter instrument, although built on the same principles, is somewhat different in detail.

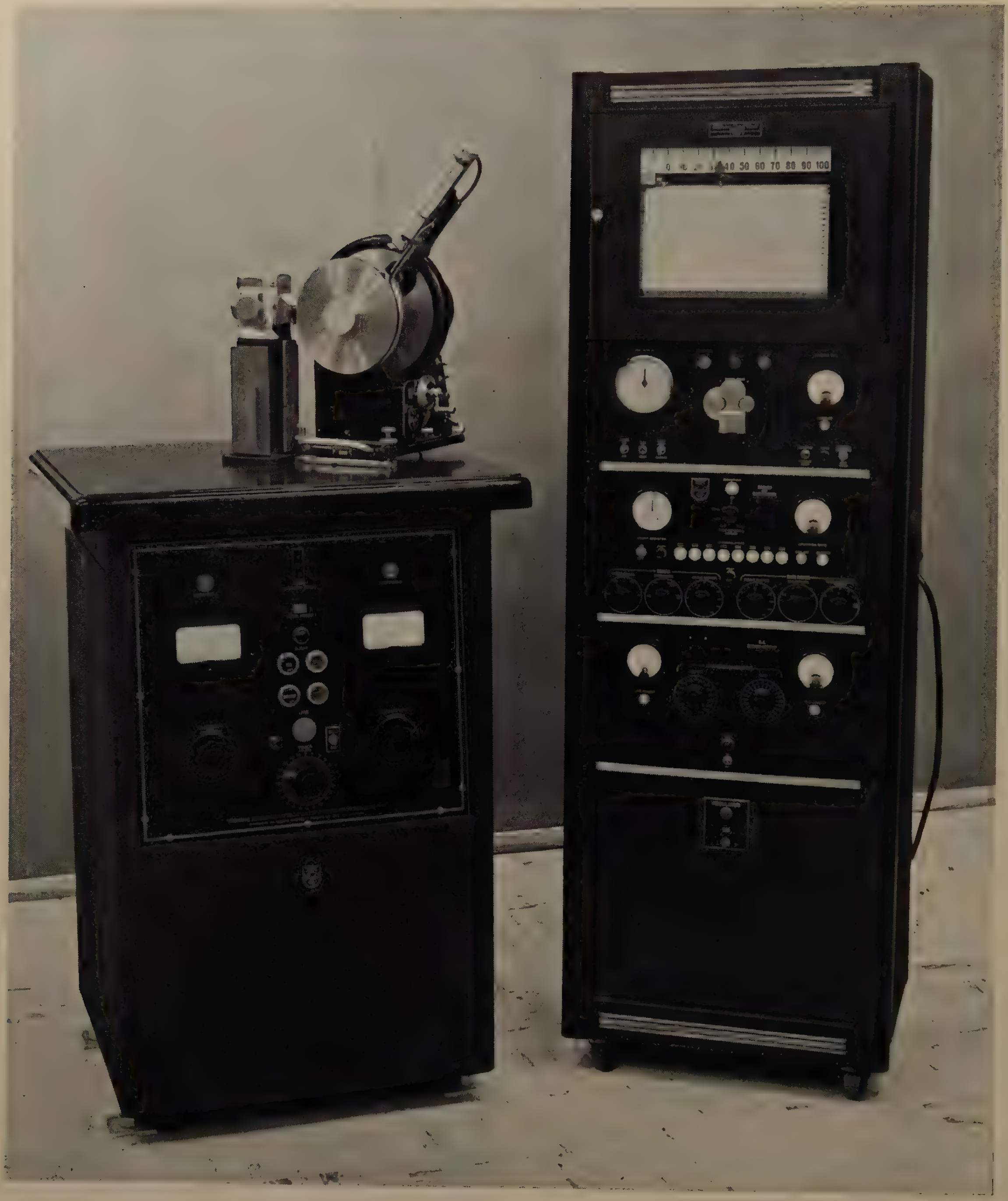

Fig. 2. The "Norelco" Geiger counter diffractometer consists of three independent parts: a basic diffraction unit (X-ray tube with high voltage generator and controls, at left), the high angle precision Geiger counter goniometer placed on top of it, and an electronic circuit rack with automatic 10″ strip chart recorder (at right).

be analysed. In the new design, however, a number of substantial improvements were obtained, which may be enumerated as follows:

1) Higher resolution in the diffraction pattern.
2) Better accuracy in the measurement of diffraction angles and line intensities.
3) Higher diffraction angle range including the "back reflection" region up to angles of $2\Theta = 165°$.
4) More universal and more flexible use of the instrument. Two goniometers and (for example) two normal photographic powder diffraction cameras can be used simultaneously in conjunction with one basic diffraction unit.

A more precise and quantitative indication of these improvements will be given below, but this short list may serve us as a guide in the description that now follows.

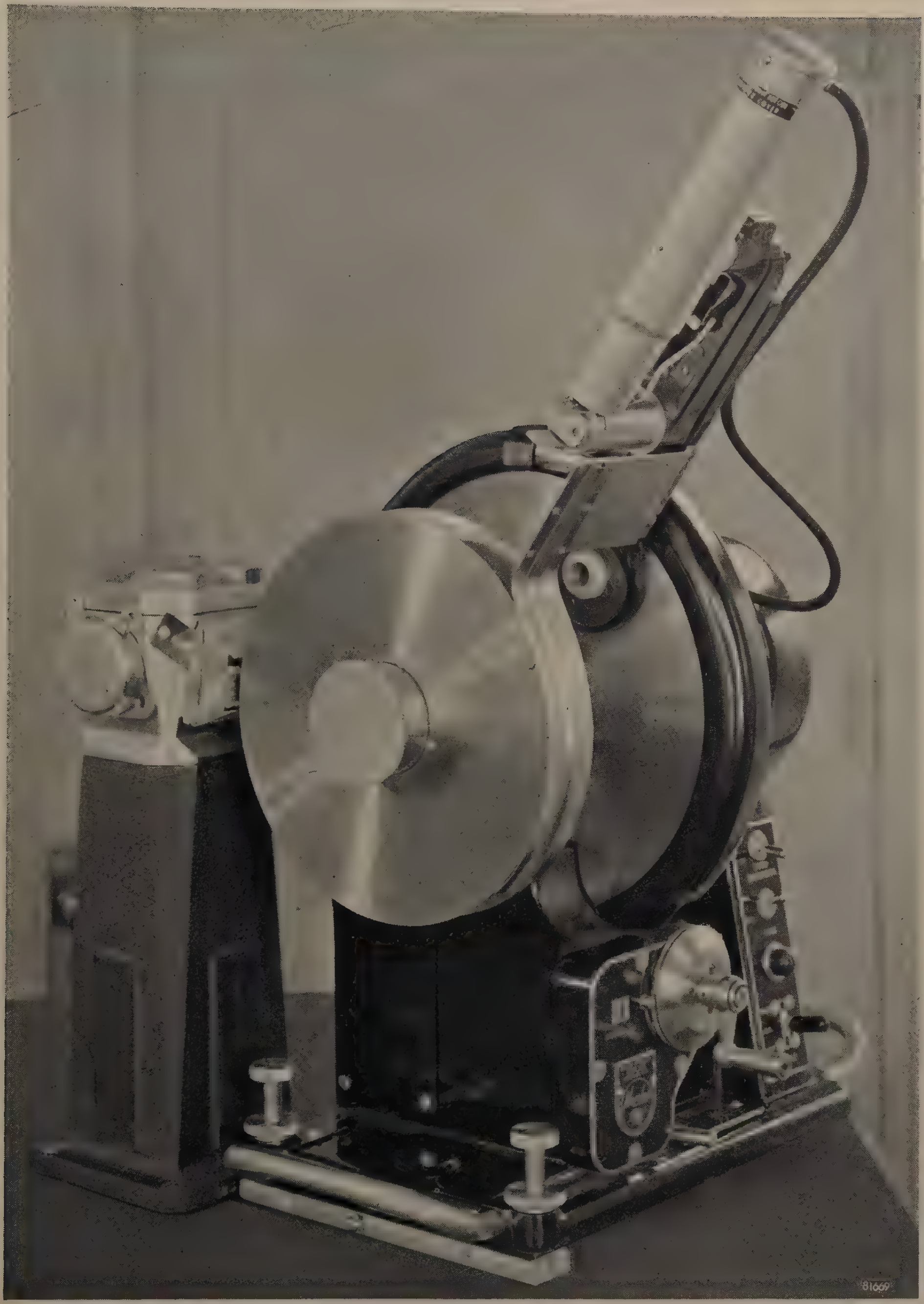

Fig. 3. The "Norelco" Geiger counter goniometer. The Geiger counter tube rigidly mounted on the scanning arm of the goniometer is seen at the top of the photograph. A handle for manual scanning and dials for reading degrees and fractions of degrees diffraction angle 2Θ are seen near the base of the instrument.

Arrangement of X-ray tube and goniometer

For the sake of clarity we start with the last point, though this improvement was obtained by rather straightforward measures, and is not necessarily the most important for all users of the instrument.

In normal photographic diffraction techniques it has been common practice for a long time to use an X-ray tube with four windows so that four diffraction cameras can be operated simultaneously. The running time of the tube and the time of the operator are thus more usefully employed. *Fig. 4* shows the arrangement. It should be noted that the windows of the X-ray tube may be divided into two pairs which transmit beams of different cross-section. The line-shaped focus produced on the target of the X-ray tube (10 mm × 1.6 mm in the "Norelco" tube) is viewed at a small glancing angle to the target surface, since at a smaller apparent size it will exhibit a higher X-ray brilliance. Through the two opposite windows looking in the *long* direction of the focus at a glancing angle of say 6°, a small, approximately square focus of 1.6 × 1.6 mm will be seen, whereas the two remaining windows looking at the same glancing angle in the direction *perpendicular* to the line focus will offer a long and very thin apparent focus, of e.g. 10 mm × 0.16 mm.

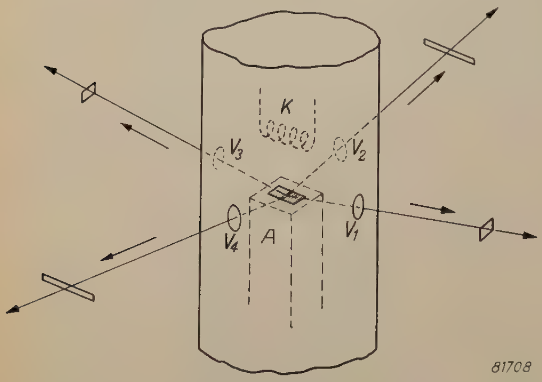

Fig. 4. Arrangement for using four diffraction devices simultaneously with a four-window X-ray tube. Through one pair of windows (spot focus windows V_1, V_2) the source is seen as a small square surface, through the other pair as a very narrow line (line-focus windows V_2, V_4). (In reality the anode A is positioned above the cathode K.)

Using the "line-focus" windows a large part of the focus area will remain unused in filling the narrow collimator sytem of a usual Debye-Scherrer camera with radiation, whereas when using the first mentioned "spot-focus" windows, radiation of the full focus area may be employed. The spot-focus windows are therefore better suited for photographic cameras such as the Debye-Scherrer and single crystal goniometers, and the line-focus windows for focussing cameras such as the symmetrical back-reflection and crystal monochromators.

In the old X-ray spectrometer both the X-ray tube and the goniometer circle, along which the Geiger counter tube travels, were mounted in a horizontal position and the X-ray optics of the arrangement was based on the employment of a "spot-focus" window (cf. the article quoted in [1])).

In the new instrument, on the other hand, the X-ray tube is mounted with its axis vertical and the Geiger counter tube scans in the vertical plane, thus offering geometrical conditions favorable for using four windows, according to fig. 4. Moreover, the X-ray optics of the present design is based on the use of a line-focus window, thus leaving the two spot-focus windows available for photographic devices. Finally, the former spectrometer for the sake of simplicity and economy contained an air-cooled X-ray tube rated for only 35 kV, 125 W; the basic diffraction unit employed with the new instrument, is equipped with a normal water-cooled X-ray diffraction tube rated for 50 kV, 800 W (copper target), which produces a high X-ray intensity, sufficient for the photographic recording of weak diffraction lines.

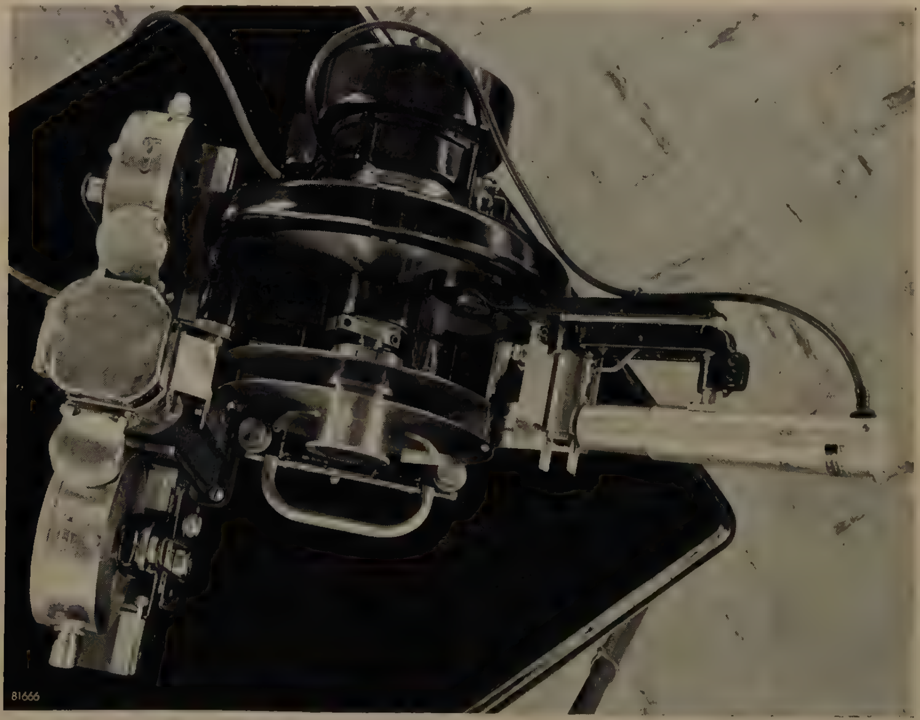

Fig. 5. Top view of basic diffraction unit, with three diffraction devices in simultaneous operation. On the left the anode end of the X-ray tube may be seen; on either side of it are two "Norelco" powder diffraction cameras; to the right is one of the new Geiger counter goniometers. Opposite the fourth window of the X-ray tube (i.e. to the far left in the photograph) another diffraction instrument can be placed.

The photograph *fig. 5* demonstrates the practicability of a simultaneous use of all four windows. In this instance one Geiger counter goniometer is used on one of the line-focus windows and two Debye-Scherrer cameras on the spot-focus windows; the fourth place is vacant.

The new X-ray optics, which is an essential innovation of the design, will presently be discussed at some length, but first it should be briefly explained how the high angular range of the diffractometer is achieved.

The high angular range

In the old instrument the angular range was limited mechanically since the movement of the Geiger counter tube beyond angles of $2\Theta \approx 90°$ was impeded by the anode end of the X-ray tube cover. With a water-cooled X-ray tube, as employed in the present diffractometer, the total anode surface required for cooling is rather small, so that the tube cover can be made to extend only slightly beyond the focus. This permits the Geiger counter tube to continue its travel to 165° 2Θ.

The increased X-ray tube rating again is essential for providing this facility, as the diffraction lines at these high angles (back reflection lines) are usually very weak.

It should be mentioned incidentally, that the useful X-ray intensity is raised not only by increasing the rating of the X-ray tube, but also by providing the tube with mica + beryllium windows instead of the formerly used Lindemann glass windows [3]. The transmission of different types of windows is indicated in *Table I*. It is seen that the transmission of mica 0.012 mm thick is about 86% for the CuKα-line (1.54 Å) which is used in most cases. The transmission of a complete window consisting of such a sheet of mica and a thin beryllium plate is about 83%. A Lindemann window 0.25 mm thick transmits only 61% of CuKα. For a softer radiation which must be used in some diffraction investigations, e.g. CrKα radiation, the advantage of the mica + beryllium window becomes even more important.

The vacuum tight mica + beryllium windows are relatively cheap and easy to fabricate, making four-window X-ray diffraction tubes an economic proposition.

Table I. Calculated transmission (%) of different types of window for X-rays of different wavelengths.

Window	X-ray spectral line	CuKα	CrKα
Lindemann glass	0.5 mm	38	5
Lindemann glass	0.25 mm	61	22
Mica	0.012 mm	86	66
Beryllium	0.12 mm	96	90
Mica 0.012 mm + Be	0.12 mm	83	60

---

[3] The use of a mica entrance window in the Geiger counter tube to give a very high sensitivity has been described in the article quoted in [1]), where the application of mica exit windows for the X-ray tube was anticipated. A description of one type of X-ray tube (contact therapy tube) equipped with a mica + beryllium window was given in Philips tech. Rev. **13**, 75-77, 1951/52.

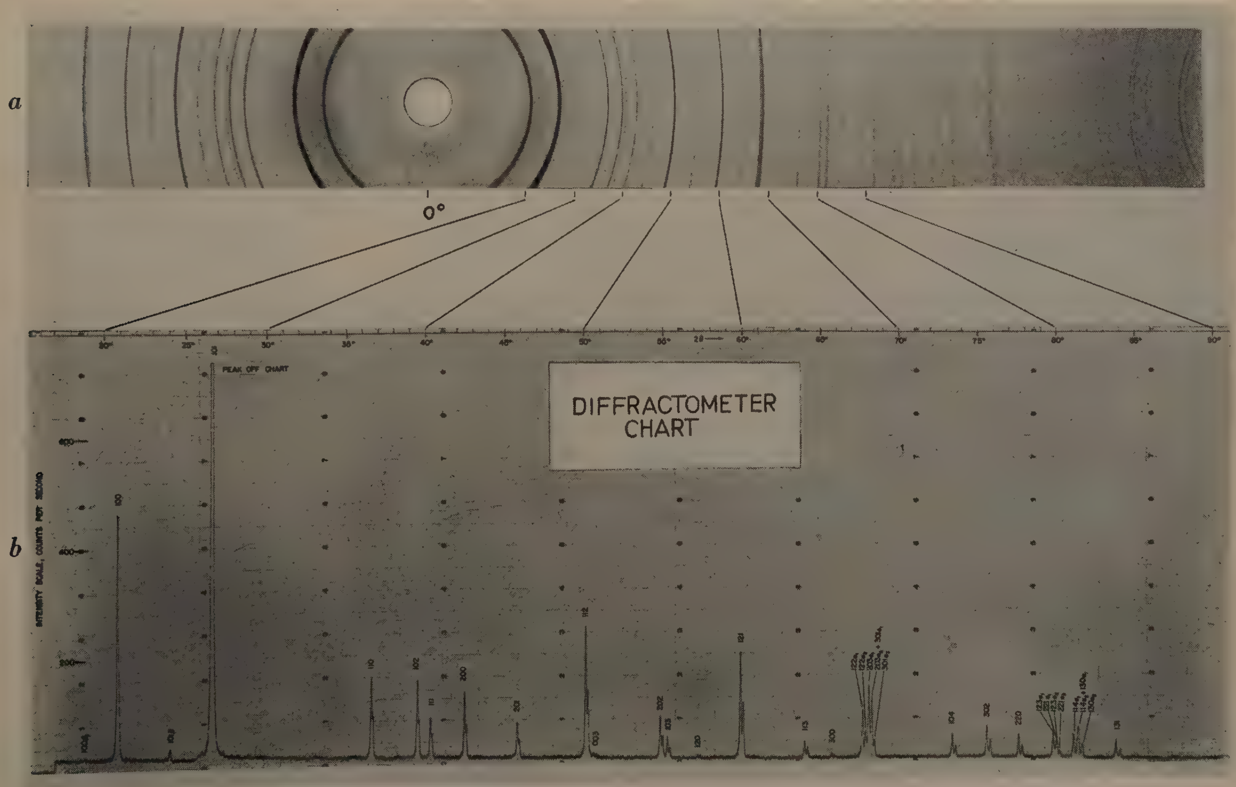

Fig. 6. *a*) X-ray diffraction pattern of quartz powder photographed with a 114.6 mm diameter Debye-Scherrer camera. Filtered CuKα radiation, 40 kV$_p$, 20 mA, exposure time 2 hours. *b*) Automatically recorded chart obtained with the new Norelco X-ray diffractometer using the same X-ray tube conditions. Recording time 4.8 hours.

X-ray optics of the instrument

Perhaps the most notable improvement obtained in the diffractometer is its very high resolution, i.e. the extreme sharpness of the diffraction lines recorded. When using CuKα radiation and recording the diffraction pattern of a well crystallized powder specimen (whose diffraction lines have a very small natural width) with a receiving slit of about the same width as the source, the width at one half peak height of the recorded Kα_1 lines is about 0.1° 2Θ in the front reflection region. The separation of the two lines produced by the CuKα_1 and Kα_2 radiations, which in normal photographic techniques can be seen only at rather large diffraction angles ($2\Theta > 110°$) is visible at about $2\Theta > 30°$ in the diffractometer recordings, cf. *fig. 6*.

This high resolution is primarily obtained by reducing the geometrical width of the X-ray source: the focus of the X-ray tube measuring 10 mm × 1.6 mm is viewed at an angle of about 3° to the target surface perpendicularly to its length (i.e. a "line" X-ray tube window is being used as stated above). The effective source width with this arrangement is 0.08 mm as against 0.2 mm in the old spectrometer. *Fig. 7* serves to illustrate the difference between the former and the present method.

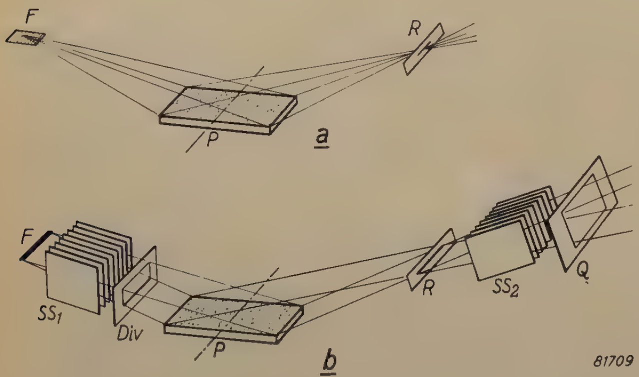

Fig. 7. *a*) X-ray optics of the former instrument (the "spectrometer" described in [1]). A "spot-focus" source *F* is used. The receiving slit *R* must be rather short in order to get a narrow recorded line profile when scanning. *P* = flat specimen. *b*) X-ray optics of the new instrument. A "line-focus" source *F* is used. The receiving slit *R* has the same length as the source. This is made possible by the use of the parallel slit systems SS_1 and SS_2, in conjunction with a chlorine quenched Geiger counter tube, as explained in the text. *Div* = aperture limiting slit, *Q* = scatter eliminating slit.

The substitution of the effective line-source in fig. 7*b* for the spot-source in fig. 7*a* was made possible by two new elements in the design, viz. the introduction of a Geiger counter tube containing chlorine as a quenching agent and the insertion of two "parallel slit systems" in the X-ray beam as shown in fig. 7*b* and *fig. 8*. Let us first consider what would happen if the parallel slit systems were omitted. The long effective X-ray source may be regarded as a large number of point-sources aligned in a horizontal direction parallel to the axis of the specimen and of rotation of the counter tube. Considering a number of imaginary vertical planes perpendicular to the axis of the goniometer, each point-source in its own vertical plane will give rise to a pattern of very narrow diffraction spots. In fact, however, owing to the horizontal divergence of the X-rays emitted from the focus each point-source will produce horizontal diffraction *lines* and thus contribute to the patterns in the planes of all the remaining point-sources. As these lines are shaped as ring sections (with a curvature largest for angles 2Θ approaching 0° and 180°, as is well-known from Debye-Scherrer photographs, cf. fig. 6*a*), the superposition of the contributions of the aligned spot-sources would result in considerable asymmetric line broadening as illustrated in *fig. 9*. This is avoided by the insertion of the two parallel slit systems, each of which consists of a number of thin (0.025 mm) molybdenum foils placed in the X-ray beam in such a way that the narrow spaces between adjacent foils may be regarded as the above-mentioned imaginary planes. Each individual spot of the line

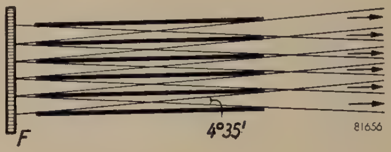

Fig. 8. Parallel slit system consisting of a number of molybdenum foils 0.025 mm thick, transmitting X-rays directed parallel to the foils and suppressing rays entering obliquely. *F* = focus. (The effect may be compared to that of the well-known Potter-Bucky grid for suppressing scattered radiation in X-ray diagnostics.)

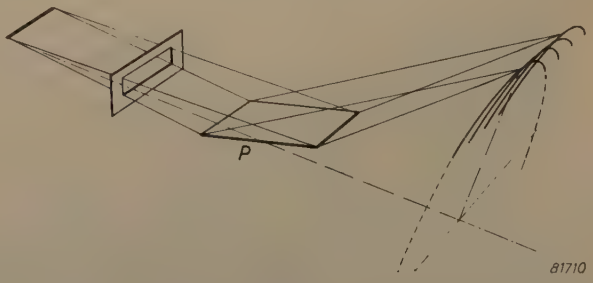

Fig. 9. If the parallel slit systems in fig. 7*b* are omitted, each point of the line source in a given specimen position produces a diffraction line of its own, covering the whole length of the counter window and being curved as a ring with its centre of curvature in the 0° 2Θ direction. The curved lines of all source points are integrated to form a broadened diffraction line of asymmetric profile.

source is now substantially prevented from contributing radiation outside its "own" plane, as these oblique radiations are strongly absorbed on their long path through the foils; the horizontal divergence of rays in each system is restricted to the very small value of 4° 35′, resulting in the very sharp lines demonstrated by fig. 6*b*. Even at small diffraction angles ($2\Theta = 5$ to 10°), where the curvature of lines is rather pronounced, the measured line profiles still have a high symmetry; see *fig. 10*.

The Geiger counter tube positioned with its window opposite a diffraction line will indicate the line intensity by integrating the X-ray energy received along the length of the line (parallel to the axis of rotation of the specimen). This is where the second factor mentioned above, i.e. the addition of chlorine to the gas filling of the counter tube, enters the picture. The tubes formerly used contained argon for absorbing the X-ray quanta (and giving rise to photo-electrons) and methylene bromide as a quenching agent. These tubes had a rather limited "sensitive volume": only those quanta that passed within about 1.5 mm from the axial anode-wire had a high probability of being counted. Hence the integration was effectively accomplished over only a 3 mm length of the line. Reflections from the whole specimen height (10 mm) were nevertheless included in this integration owing to the rather large horizontal divergence permitted. With the X-ray optics of the goniometer illustrated in fig. 7*b*, however, the limitation of the line length to 3 mm at the entrance of the Geiger counter tube would mean that reflected rays emanating from the ends of the specimen surface are not detected and that the ends of the X-ray source do not contribute to the integrated line intensity. It is an essential feature of the revised X-ray optics that the chlorine counter tubes possess a much larger sensitive volume, covering the complete 10 mm width of the beam in the goniometer (*fig. 11*): this ensures that full use is made of the focus as well as of the specimen area (the latter is important for good averaging of the crystallite reflections).

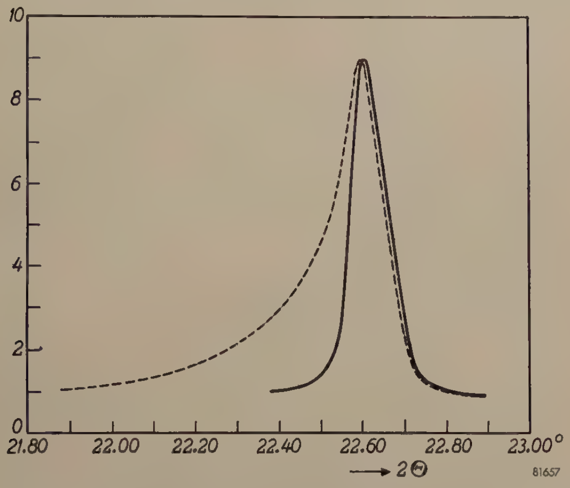

Fig. 10. Profile of a diffraction line measured with the Geiger counter diffractometer, without the parallel slit systems (broken line) and with the parallel slit systems (full line).

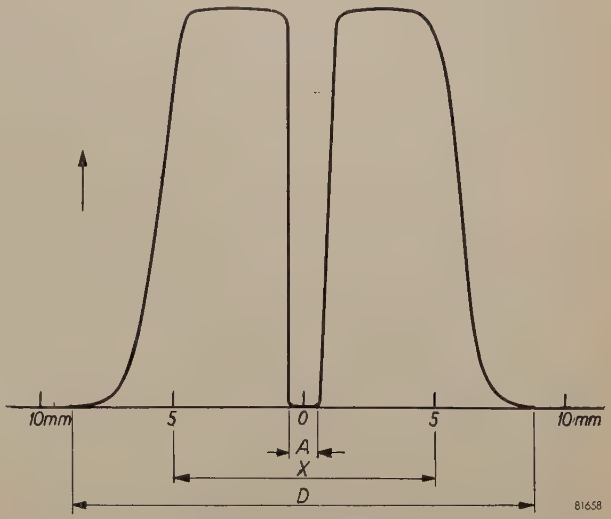

Fig. 11. Radial distribution of sensitivity (in arbitrary units) of chlorine-quenched Geiger counter tube (type 62019). A = width of the axial anode wire and bead. X = width of X-ray beam when using the new X-ray optical system. D = inside diameter of the Geiger tube.

The chlorine counter tubes also offer other advantages: for example, a very long life, a rather low working voltage and a long "plateau", but we shall not dwell on these points in this article [4]). A photograph of the counter tube in its present form is reproduced in *fig. 12*.

Although the Geiger counter tube in its present form has excellent characteristics as a radiation detector, other types of detectors have been developed for use in the diffractometer, viz. special forms of the proportional counter and the scintilla-

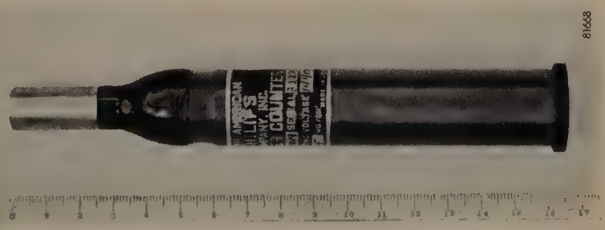

Fig. 12. The Geiger counter tube, type 62019, used in the "Norelco" diffractometer. The end window where the X-rays enter the tube (in a direction parallel to the tube and its axial anode wire) is made of mica 0.012 mm thick. The gas filling consists of argon to a pressure of approximately 55 cm Hg with a few mm Hg chlorine as a quenching agent. The operating voltage is 1400 to 1500 volts, the plateau is at least 300 volts long.

---

[4]) See N. Warmoltz, Geiger Müller counters, Philips tech. Rev. **13**, 282-292, 1951/52.

tion counter. Both of them have the advantage of a very short "dead time", allowing counting at rates many times higher than with the Geiger counter. Moreover, they offer the possibility of pulse height discrimination, which in some cases may be useful. An example is the X-ray diffractometry of radioactive samples, where the background caused in the diffraction pattern by the radioactivity can be reduced very effectively when using a scintillation counter [5]). The latter has a higher quantum efficiency than all other radiation detectors (nearly 100%) for the wavelengths normally used in X-ray analysis.

It is interesting to compare the old and the new instrument from the viewpoint of the number of counts per second obtained for a given diffraction line. It should be pointed out that with a given real focus area a crystallite of the specimen "seeing" the whole focus will receive the same radiated energy per second regardless whether the focus is viewed from its broad or from its narrow side and whatever viewing angle is chosen [6]) (within certain limits). This well known basic fact would mean in our case that the increased resolution would not entail a sacrifice of line intensity except in so far as the horizontal divergence of the rays has been somewhat decreased, permitting a crystallite to see only part of the focus. This loss, however, is amply made good by the much higher radiation output per cm² of the focus (higher specific loading of the focus made possible by the water-cooling).

The goniometer; alignment procedure

In order to obtain full profit from the high resolution achieved it was necessary to ensure that diffraction angles could be measured with adequate accuracy. A large goniometer radius was therefore chosen (radius 17 cm instead of 13 cm with the former instrument [7])), resulting in a large dispersion of the diffraction pattern. At the same time a completely new mechanical design was adopted for the goniometer, enabling the setting and direct reading of the Geiger counter tube position to an accuracy of 0.01° 2Θ or better.

A cross-section drawing of the goniometer is shown in *fig. 13*. It consists essentially of a precision 10″ worm wheel and worm drive (W_1 and W_2). The wheel carries the Geiger counter tube rigidly attached to it in a radial position. The main dial permitting direct reading of 2Θ to 0.01° is fixed on the worm, complete dial revolutions being registered by a subsidiary gear and a mechanical counter. This accuracy is achieved by "cold working" the wheel and permanently loading the worm against it [8]). The specimen under investigation, which is made in the shape of a flat plate 20 × 10 mm (P in fig. 13), is placed in a holder carried by a hollow shaft positioned within the hollow bearing of the worm wheel and coupled to the latter by a set of accurate herringbone gears. These rotate the specimen at exactly one-half the angular speed of the Geiger tube arm.

To ensure the above-mentioned accuracy of the diffraction angle measurements, the zero angle position of the goniometer must be set to a precision of better than 0.01° 2Θ. This is achieved as follows. A narrow slit or pin-hole is placed in the specimen holder (*fig. 14a*). The reference or banking surface of the holder contains the specimen rotation axis, which is made in the factory to coincide with the goniometer axis to better than 0.01 mm. The goniometer arm is turned slowly in 0.01° steps across the X-ray beam transmitted by the slit or pin-hole. The position of maximum intensity thus found is the zero angle position, provided the slit was placed

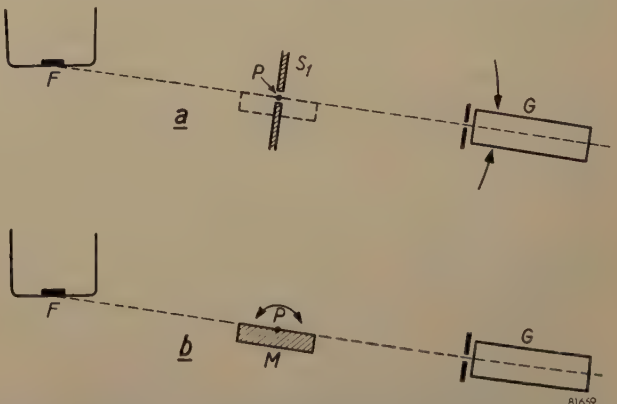

Fig. 14. Alignment and calibration procedure for the goniometer. *a*) A narrow slit S_1 is placed at the specimen rotation axis *P*. The Geiger counter tube *G* is turned to the position in which the largest intensity of the direct X-ray beam transmitted by S_1 is recorded (*F* = focus of X-ray tube). This is the zero angle position of the goniometer.
b) A flat machined piece of metal *M* is fastened on the specimen holder and rotated so that maximum intensity of the direct X-ray beam is received by the Geiger counter tube in its zero angle position. The specimen reference plane is then exactly parallel to the zero angle direction, and the exact ratio 1:2 of specimen angle and counter tube angle is obtained when scanning.

---

[5]) T. R. Kohler and W. Parrish, X-ray diffractometry of radioactive samples, to be published in Rev. sci. Instr. Cf. also: J. Taylor and W. Parrish, Absorption and counting efficiency data for X-ray detectors, also to be published in Rev. sci. Instr.

[6]) This is due to the fact that the impinging electrons penetrate only very slightly into the target whereas the X-rays produced at a depth where the electrons are stopped emerge from the target practically unimpeded even in directions nearly parallel to the target surface. Thus from all directions (in front of the target) the same *volume* of target material is seen to contribute to the radiation. See for example Philips tech. Rev. **3**, 261, 1938.

[7]) It should be remembered that most diffraction cameras have *diameters* of 5.7 or 11.4 cm. Increasing the radius beyond 17 cm did not seem desirable because of increasing air absorption for long wavelengths and air scatter; moreover, at 17 cm, the size of the instrument is still reasonable.

[8]) This process is conducted in such a way that the resultant surface hardening almost eliminates further wear.

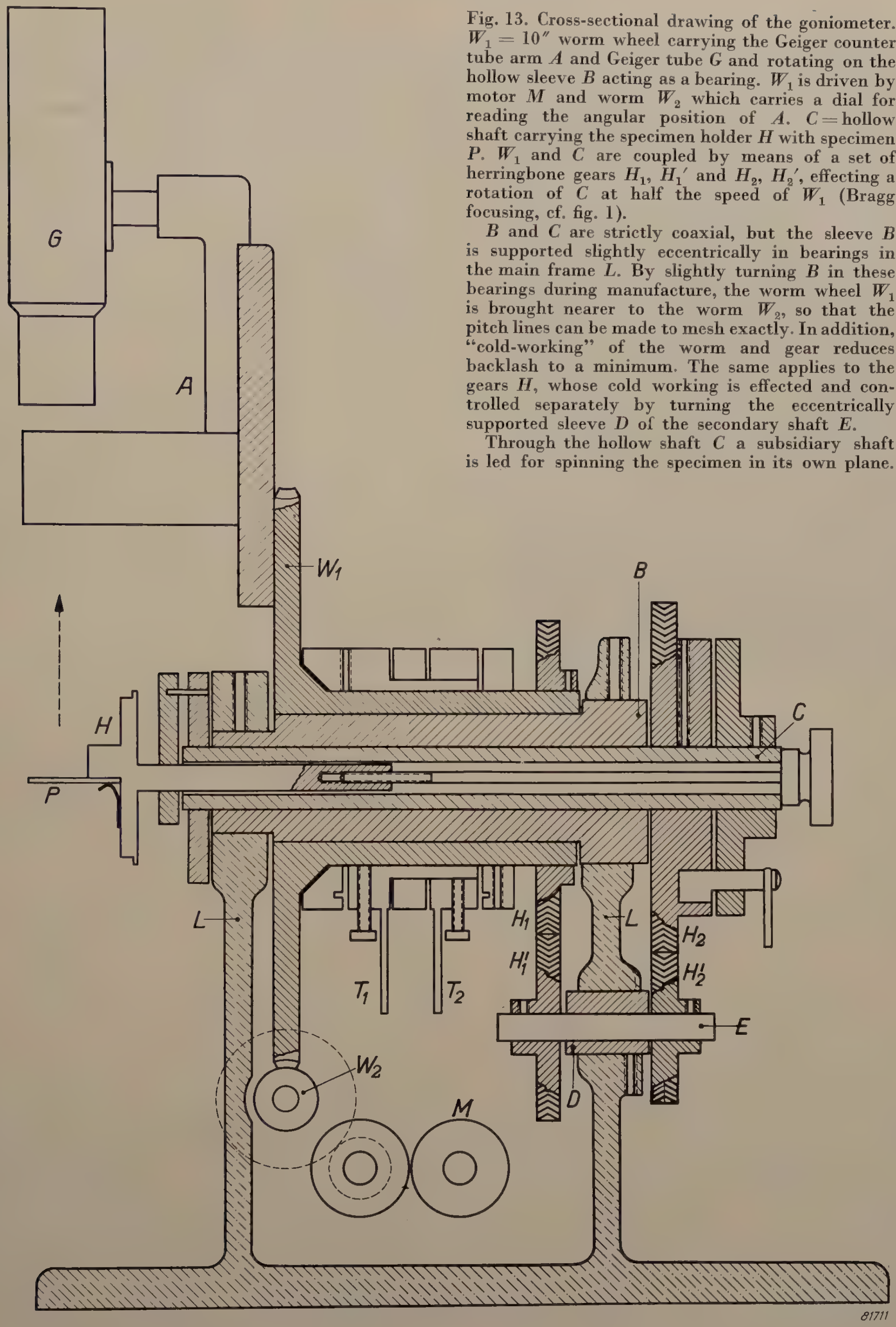

Fig. 13. Cross-sectional drawing of the goniometer. $W_1 = 10''$ worm wheel carrying the Geiger counter tube arm A and Geiger tube G and rotating on the hollow sleeve B acting as a bearing. W_1 is driven by motor M and worm W_2 which carries a dial for reading the angular position of A. C = hollow shaft carrying the specimen holder H with specimen P. W_1 and C are coupled by means of a set of herringbone gears H_1, H_1' and H_2, H_2', effecting a rotation of C at half the speed of W_1 (Bragg focusing, cf. fig. 1).

B and C are strictly coaxial, but the sleeve B is supported slightly eccentrically in bearings in the main frame L. By slightly turning B in these bearings during manufacture, the worm wheel W_1 is brought nearer to the worm W_2, so that the pitch lines can be made to mesh exactly. In addition, "cold-working" of the worm and gear reduces backlash to a minimum. The same applies to the gears H, whose cold working is effected and controlled separately by turning the eccentrically supported sleeve D of the secondary shaft E.

Through the hollow shaft C a subsidiary shaft is led for spinning the specimen in its own plane.

exactly on the goniometer axis. The unavoidable error in the placing of the slit is compensated by repeating the procedure with the specimen holder revolved through 180°. The mean value of the two maximum intensity positions read is the true zero angle position. With the arm in this position, the dial is unscrewed and reset to 0.00°.

When this has been done, the specimen holder in this goniometer position must be adjusted so that the surface of the flat specimen will be exactly parallel to the zero angle direction, in order that this surface on scanning will always be oriented at *exactly* one-half the angle of the Geiger counter tube arm (cf. fig. 1). This so-called 2:1 setting is performed (with the goniometer arm set at 0.00°) by placing a flat machined piece of metal in the specimen holder (fig. 14*b*), and rotating the holder by means of a micro-adjustment until maximum intensity of the direct X-ray beam is obtained.

As was mentioned above, the reference surface of the specimen holder is manufactured so that it coincides with the goniometer axis to better than 0.01 mm. If diffraction occurs only at the specimen surface, which is approximately the case for a strongly absorbing material, and if the specimen were removed only 0.075 mm from the axis of rotation, the peak positions of the diffraction lines would be shifted 0.045° 2Θ at $2\Theta = 45°$.

Relative line intensity measurements

Since the Geiger counter method of recording X-ray diffraction patterns (unlike the film method) requires point-by-point measurements, the intensity of the primary X-ray beam must be highly stabilized to make relative measurements of the diffracted intensity reliable. The X-ray generator of the basic diffraction unit employed now operates on full wave rectified voltage enabling more reliable regulation than the previous instrument with a self-rectifying X-ray tube. Long term stabilization to better than 0.2% for both voltage and current of the X-ray tube is obtained by use of an electronic voltage regulator and a feedback type current regulator [9]).

Intensity measurements for weak lines are facilitated by the wavelength response of the argon-filled Geiger counter tube, as was discussed in the article quoted above [1]); the background intensity of the diffraction pattern due to the short wavelength continuous radiation is detected with a relatively low efficiency, resulting in a low and even background, comparing very favorably with that of photographically recorded patterns, for equal line peak height. The recording and measuring of weak lines is further improved by the higher intensity of the water-cooled X-ray tube. It is important to note that better accuracy of the intensity measurement is achieved also for *strong* diffraction lines, owing to the full wave rectification. It is well known that for the comparison of high and low line intensities, the non-linear response of the Geiger counter tube, which is caused by the "dead-time" after every recorded count, is an fundamental limitation. By using full wave instead of half wave rectified voltage across the X-ray tube, with the same total number of quanta arriving in a random fashion at the Geiger counter tube the average time-separation of two quanta will be doubled, thus diminishing the influence of quanta arriving in "dead time" periods and hence shifting the non-linearity effect to higher intensities (twice the former limit).

If line intensities in different 2Θ regions have to be measured, the differences of illumination of the 20 mm width of the specimen rotating in the fixed primary beam must be taken into account. With a beam of angular aperture 1° in the scanning plane, the 20 mm specimen width is just covered when the specimen is positioned at 17° 2Θ. As the angle increases, only part of the specimen is illuminated. This does not affect the relative line intensities, provided the sample is of sufficiently uniform reflecting power over its whole surface. For accurate measurements we have found it useful to rotate the specimen in its own plane (at moderate speed, e.g. 77 rev/min) in order to smooth out the statistical fluctuations obtained even with crystallites smaller than 20 μ in the specimen. Such a rotation is performed by means of a subsidiary shaft led through the hollow specimen holder shaft (*C* in fig. 13) of the goniometer and driven by a motor placed at the rear of the instrument. In this way congestion around the specimen is avoided and enough clearance is provided for mounting high or low temperature specimen chambers or other accessories.

In order to make use of the whole specimen surface in the back reflection region, where line intensities are very low, the angular aperture of the primary beam is increased to 4° by inserting a larger aperture-limiting slit. On the other hand, for small Bragg angles, $2\Theta < 17°$, smaller apertures must be used, so that the beam does not exceed the specimen width. (This is desirable even when line intensities are not to be measured, in order to avoid excessive scattering. With very small apertures, down to 5′, it is thus possible to measure diffraction angles corresponding to lattice spacings up to about 90 Å, using CrKα radiation.) The divergence slits, as well as the other slits shown in fig. 7*b*, are designed for maximum reproducibility and convenience by having *fixed* apertures. All slits are constructed of molybdenum, for high X-ray absorption and good mechanical strength.

Scanning of the pattern; counting methods

It will be remembered that due to the random arrival of quanta the accuracy of the line intensity measurement depends on the total number of counts recorded by the Geiger counter tube when traversing the angular region of the diffraction line [1]). In order to conform to specific accuracy requirements, different counting methods can be adopted. With the simplest method, which is used for most routine analyses, and for recording charts as in fig. 6*b*, the pattern is continuously scanned and the average current intensity produced by the current pulses of the Geiger tube is measured. Automatic scanning is accomplished by driving the goniometer by a fractional horsepower electric motor (M in fig. 13). A contact on the main worm shaft of the goniometer with a cam for 0.5° intervals in 2Θ actuates a degree marking pen on the strip chart recorder. The accuracy of the recorded line intensities depends on the scanning speed. Through the use of changeable spur gears, scanning speeds (in either direction) of $^1/_8$, $^1/_4$, $^1/_2$, 1 or 2° per min can be selected. A wider receiving slit is used for scanning at higher speed in order not to lose too much in intensity. Owing to the high X-ray intensity of the tube the accuracy is fairly good even at the highest scanning speed. The chart reproduced in fig. 6*b* was recorded at medium speed ($^1/_4$°/min); the recording took about 5 hours.

---

[9]) The Eindhoven version of the diffractometer employs a specially designed basic diffraction unit (type PW 1010) containing a more elaborate stabilization device.

The same method can be employed for investigating only small parts of a diffraction pattern. Use is then made of adjustable upper and lower limit stops provided on the goniometer (T_1 and T_2 in fig. 13) for stopping or reversing the scanning motion.

For higher accuracy, manual point-by-point plotting of a chart, using the so-called fixed count method, is sometimes desired. In this case a discontinuous stepwise movement of the goniometer is substituted for the continuous scanning movement. The mechanism causing this stepwise movement is shown in *fig. 15*. It can be adjusted to advance the Geiger counter tube in steps from 0.01° to 0.05°2Θ. This type of scanning motion is required also for the recording *counting rate computer*, a device developed to combine the advantages of fully automatic operation and high accuracy in a wide range of intensities.

For the sake of completeness a fourth method of obtaining data from the goniometer should be mentioned, viz. the integrated area measurement. This method and the other methods mentioned above will be described in detail in a subsequent article. All the circuits necessary for measurements according to these methods are contained in the cabinet shown on the right of fig. 2. The conversion from one method to another can be done simply and quickly by means of tap switch selectors.

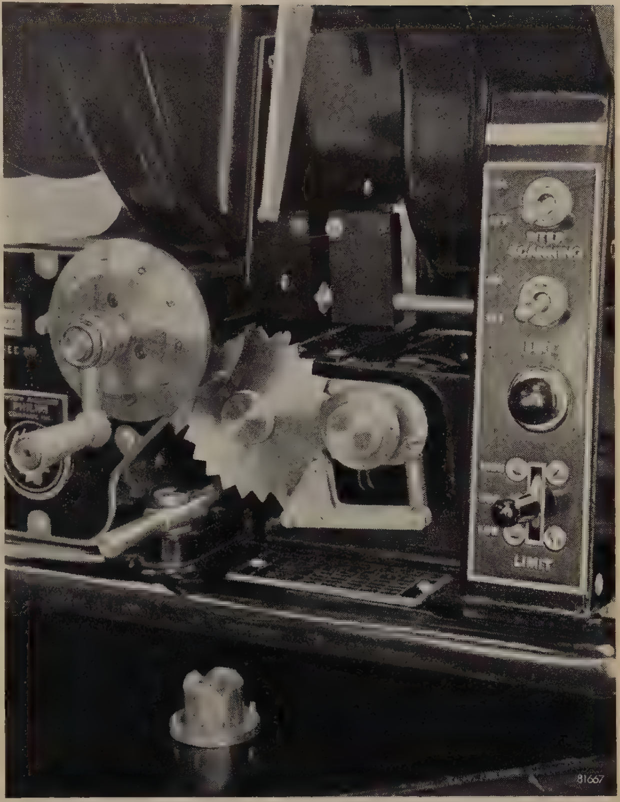

Fig. 15. Mechanism for stepwise movement of the goniometer arm. The goniometer arm rotates through 0.25° for each revolution of the shaft geared directly to the motor. For the stepwise movement this shaft is fitted with a wheel with 25 triangular-shaped teeth which is advanced one tooth at a time by a pin on the driving member on the motor shaft. With one pin on the driving member one revolution of the motor shaft advances the goniometer by 0.01° 2Θ, with two pins 0.02°, etc. The driving member can accomodate up to 5 pins (see driving member in the foreground). Indexing is achieved by a spring loaded roller which falls between the teeth of the wheel.

Summary. The "Norelco" X-ray diffractometer, which has now been commercially available for some years, is a completely re-designed version of the Geiger counter X-ray spectrometer formerly described in this Review. The new version incorporates an improved resolution of diffraction lines ($\mathrm{CuK}\alpha_1$-α_2 separation visible at $2\Theta > 30°$), better accuracy in the measurement of diffraction angles (readings to 0.01° in 2Θ) and of relative line intensities, ansd a higher diffraction angle range (up to $2\Theta = 165°$). These improvements are due to the use of a new X-ray optical system together with a normal basic diffraction unit having a high-powered water-cooled X-ray tube with mica-beryllium windows, and to the design of a high precision mechanical Geiger counter goniometer. The new X-ray optics is based on the use of a line-focus source. Owing to this feature and to a vertical arrangement of the X-ray tube and goniometer circle, it is possible to use two goniometers and two normal photographic powder diffraction cameras simultaneously with the four window X-ray tube of one basic diffraction unit. Scanning speeds varying from $^1/_8$° to 2° per minute can be selected; alternatively an automatic stepwise movement of the goniometer is possible. Apart from automatic recording, either continuously or point-by-point, the electronic circuits developed for the instrument permit the application of special counting methods. The various counting and recording methods will be described in a following article.

A POCKET DOSEMETER, WITH BUILT-IN CHARGER, FOR X-RADIATION AND GAMMA RADIATION

by N. WARMOLTZ and P. P. M. SCHAMPERS.

621.386.82 : 539.16.08

The accumulated dose of γ-radiation and X-radiation to which a person has been exposed is commonly determined by means of a miniature ionization chamber combined with an electroscope charged to some hundreds of volts, which can conveniently be carried in the pocket. In this type of instrument the radiation causes discharge of the system according to the dosage; this can be read from the electroscope by means of a microscope provided for the purpose; Thanks to new developments in glass technology, however, it is now possible to make these dosemeters completely vacuum-tight and able to withstand higher voltages, which increaese the deflection and so permit the microscope to be dispensed with. Moreover, it is found that this construction is well suited to the incorporation of an electrostatic charger in the same instrument; this does away with the need of batteries and enables the meter to be used under any conditions, even under water.

Ionizing radiations

Effect upon living tissue

Owing to the present large-scale production of artificial radioactive substances, ionizing radiations other than the familiar X-rays are being produced. For example, γ-rays are now being generated on a wide scale and at intensities which at one time would have been considered incredibly high: hence the problems relating to the effect of these radiations upon living organisms are demanding more and more attention.

In view of these developments, the measurement of the dosages to which people are exposed is a subject of considerable importance. Before entering into the details of this subject, however, we will briefly recall the manner in which these radiations affect biological matter and the methods adopted to establish a measure of the irradiation dose based on these biological effects.

Charged particles, e.g. α-rays, β-rays, protons and fission products, cause direct ionization and also excitation and dissociation of molecules. In matter, they proceed along a certain path depending, amongst other things, upon the energy, mass and charge of the incident particle and the nature of the particular material through which it passes. The depths of penetration of these particles with the energies nowadays prevalent are relatively small, ranging from some fractions of a millimetre to a few centimetres in the case of very hard β-radiation.

On the other hand, X-ray and γ-ray quanta (photons) cause very little direct ionization, but the fast electrons released by these quanta have, like β-radiation, a very high ionizing power, and so cause secondary ionization, excitation and dissociation.

For these electromagnetic quanta the probability of absorption is considerably less than for the first-mentioned particles, so that, in general, the rays pass right through the object, though attenuated by scatter and absorption. To illustrate this point, 1 MeV γ-radiation in water has a linear coefficient of absorption of 0.07 cm^{-1}: in other words, this radiation is reduced to about $^1/_3$ of its original intensity in penetrating a barrier of water about 14 cm thick.

Fast neutrons, being uncharged, ionize indirectly by transferring a considerable proportion of their energy to any light-weight nuclei with which they happen to collide, so enabling these nuclei to produce ions in the tissue. Slow neutrons cannot do this, but in certain substances readily produce nuclear reactions whereby ionizing particles are released. The penetrating power of fast neutrons is very high in heavy substances, but decreases with the weight of the atoms constituting the material.

Dosimetry

To study the effect of radiation upon biological matter we require in the first place a measure of the radiation. Let us now consider the manner in which such a measure is established.

The processes initiated by radiation in biological tissue are very complex as may be deduced from the fact they involve such subsidiary effects as the above-mentioned ionization, excitation and dissociation; in fact, there can be no doubt that our concept of these processes as a whole is still incomplete. However, it has been found in the course of many investigations that the quantity of energy absorbed may be employed as a measure of the effects produced by radiation, for example, the destructive effect upon tissue. Since direct measurement of the energy absorbed by a particular tissue is usually impracticable, it is necessary to find some other means of obtaining this information. An associated quantity suitable for direct measurement is the ionization caused by the radiation in a given volume of air (or other gas).

Since the mean energy to form one ion pair in air is known (32.5 eV), the energy absorbed in the air can then be computed. To ascertain from this the amount of energy absorbed in a particular tissue, it is necessary to take into account the nature of the tissue and that of the radiation, and the geometry of the object and of the beam.

The energy absorbed by a particular tissue can be computed for a wide range of wavelengths of X-rays and γ-rays by multiplying the corresponding value in air by the ratio of the respective X-ray absorption factors of the two absorbers [1]). The unit of dosage employed for X-radiation and γ-radiation is the röntgen: one röntgen of X-radiation or γ-radiation is such that it produces in 0.001293 gram of air (1 cc at 1 atm. and 0 °C) ions of either sign carrying 1 e.s.u. of charge. The amount of energy absorbed by air from one röntgen (r) is 84 ergs per gram.

It is particularly necessary to bear in mind that, in general, the value in röntgens is merely a measure of the X-ray irradiation at a particular point, as evaluated in terms of the ionization caused by such irradiation assuming that there is air at that point. This applies irrespective of the real nature of the matter constituting the point concerned. However, throughout a wide range of wavelengths the röntgen-evaluation is likewise a measure of the effect produced by the radiation. It is found that the amount of energy absorbed per röntgen varies very little as between different biological tissues; for the most important muscle, and other tissues, the energy absorption at nearly all wavelengths is 80 to 100 ergs per gram per röntgen.

However, for relatively soft radiation some tissues absorb considerably less energy (e.g. up to 50 ergs per gram per röntgen in the case of fat) and others considerably more (roughly, up to 500 ergs per gram per röntgen).

Basically, the equipment employed to measure radiation in röntgens comprises an air-filled chamber containing two electrodes between which a voltage is applied, and a sensitive instrument for the measurement, either direct or indirect, of the ionization current [2]).

For β-particles and other radiations which cannot conveniently be measured in röntgens and to which the formal definition of this unit is not strictly applicable, another quantity has been introduced, i.e. the "absorbed dosage", the unit of which is the "rad". The "absorbed dosage" may be defined as the amount of energy transferred from an ionizing radiation to a particular point in a given substance per unit mass by ionizing particles. One rad is equivalent to an absorbed dosage of 100 ergs per gram; X-radiation can also be evaluated in terms of the rad.

Although in general the effect of a particular radiation upon organic tissue depends upon the dosage as measured in röntgens or rads, equal rad-dosages of different radiations do not always produce exactly the same biological effect. Owing to the complexity of the process it is impossible to assign this difference direct to any particular cause, but there is little doubt that it arises from spatial variations in ion density. For example, where an α-particle and a β-particle cause the same overall ionization, the one will produce along its relatively shorter path a much greater concentration of ions than the other. Again, fission products and recoil nuclei of neutrons likewise produce very heavy ion-concentrations as compared with β-particles, or with X-rays and γ-rays. This relative concentration of the ionization sometimes enhances, and sometimes diminishes the biological effect.

Accordingly, another unit has been introduced, viz. the "rem". A dosage in rems equals the same dosage in rads multiplied by a factor representing the relative biological effect appropriate to the particular case. As a rule, tolerance dosages are expressed in terms of the number of rems per week. According to definition, the relative biological effect of X-radiation and γ-radiation is unity; hence the tolerance evaluated in rads equals the tolerance in rems. We have already seen that in certain (usually unimportant) circumstances, the energy absorbed per röntgen by particular tissues may vary quite appreciably above or below 1 rad; however, for purposes of protection against X-radiation and γ-radiation, where the precise maximum tolerance dose is not always known, this possible variation is ignored and 1 röntgen is considered equivalent to one rad.

The measurement of X-radiation and γ-radiation can also be accomplished by means of a suitable Geiger-Müller counter, crystal counter or scintillation counter, and the result expressed in terms of the number of particles so recorded per unit area and per unit time. Provided that the sensitivity of the particular counter and the energy distribution of the radiation are known, the dosage in röntgens can then be computed.

---

[1]) For a more detailed account of these effects and of the exact method of measurement, see the article by W. J. Oosterkamp in Appl. sci. Res. **B3**, 100, 1953 and **B3**, 477, 1954.

[2]) See the article by J. van Hengel and W. J. Oosterkamp in Philips tech. Rev. **10**, 338 - 346, 1948/49.

Another widely-used method of dosimetry is that based upon the blackening of a photographic plate. Again, the discoloration or fluorescence of certain crystals and glasses has lately been adopted as a measure of large dosages.

Tolerance dose

It has long been evident that exposure to X-radiation or γ-radiation causes varying degrees of damage to living organisms. The effects increase in severity with the dose, ranging from small changes inaccessible to direct observation, and slight and temporary variations in the blood count, to grave, possibly fatal, injuries to essential organs. Similar effects are produced by corpuscular radiations, the least penetrating of which, although affecting only the skin and the subcutaneous tissue, may nevertheless give rise to serious consequences.

The increasing use of radioactive substances and ionizing radiations in science and technology calls for the provision of a survey of tolerance dosages. Accordingly, the International Commission on Radiological Protection has recommended certain maximum limits for the radiation doses which may be considered tolerable in the event of life-long irradiation of the entire body (*Table I*).

Table I. Tolerance dose for irradiation of the entire body.

	X-radiation or γ-radiation	Other ionizing radiation
In the blood-forming organs, sex organs and the eyes . . .	0.3 r or rad per week	0.3 rem per week
In the base layer of the epidermis . . .	0.6 r or rad per week	0.6 rem per week

For irradiation confined to the hands and forearms, the feet and ankles, or the head and neck 1.5 r per week is permissible, provided that in the last case the eyes are protected so that the dose received by them does not exceed 0.3 r per week.

Since α- or β-radiations and protons can usually be prevented from reaching the body by quite simple methods (e.g. gloves), the above tolerances are important first and foremost in work involving X-radiation, γ-radiation and neutrons; on the other hand, substances emitting α-radiation are particularly dangerous when assimilated through the nose or mouth.

All the tolerances are specified in terms of the dosage per week. It is held to be immaterial whether the dose absorbed during this period results from a brief irradiation at a high dosage rate, or from a continuous irradiation at a low one. The effect of the radiation upon living tissue is cumulative, but partial recovery takes place in the course of time.

To complete this survey, *table II* shows the approximate effects of a large short-period dose of γ-radiation under conditions of total body irradiation.

Table II. Effect of a heavy short-period dose of γ-radiation, body totally irradiated.

0- 25 r : no perceptible injury.
25- 50 r : changes in the blood count, no serious injury.
50-100 r : changes in the blood cells, some injury.
100-200 r : serious injury.
200-400 r : very grave injury, possibly fatal.

Pocket dosemeters for personal protection

In order to avoid the danger of exceeding the tolerance doses defined above, a person working in the presence of ionizing radiations must acquire, with the aid of one of the usual instruments for measuring dosage rate, an appreciation of the situation in which he works and hence an assurance that in normal circumstances he will not absorb more than the permissible weekly dose. Since he cannot continuously measure the dosage rate prevailing wherever he happens to be throughout the day, and since this rate usually varies at every moment, it is desirable that the worker be provided with a pocket dosemeter from which he can read, at the end of a day or week, the total dose absorbed during that time. This also ensures that any incidental and transient increase in intensity will be measured as well.

Where the particular radiation employed is confined to a narrow beam, special precautions are necessary to ensure that this beam cannot strike any part of the body without also striking the dosemeter.

Dosemeters of the type usually employed include a very thoroughly insulated electrometer system, which is charged from a battery or some other source of about 200 V; the deflection of this meter is read with the aid of a small microscope. The electrometer system is encased in a conductive housing, which also constitutes the ionization chamber containing air at a pressure of 1 atm. The number of ions formed in this chamber per second by the incident radiation corresponds to the dosage rate, and the total number of ions so formed during the particular period of observation governs the discharge of the system. As a rule, the displacement of the electrometer leaves is proportional to this total, and the dosage can be read from the scale of a microscope calibrated in röntgens.

One of the existing types of dosemeter has a sensitivity of 0.5 r full scale deflection; the variation in the reading of this meter in the absence of radiation is only 1 to 2% per 24 hours. Heavier doses are measured by means of dosemeters incorporating well-insulated capacitors, which increase the full scale deflection reading to 100 r. A diagram of such a meter is shown in *fig. 1*.

A simple charging device incorporated in the instrument would enable the latter to be used as a dose-rate meter, from which the time required for a discharge covering a certain number of scale divisions can be determined by counting. Although by no means comparable in quality with the instruments usually employed for this purpose, the above combination would constitute a very simple and inexpensive dose-rate meter. A meter of this type giving a full scale reading of 0.2 r would permit a dosage rate of 72 röntgens per hour to be measured quite easily in a matter of 10 seconds, again, a rate as low as 2 r per hour could be measured with the same instrument in 1 minute by utilising only about 20% of the scale. Higher dosage rates, up to the order of several hundred röntgens per hour, could also be measured with the same instrument. However, to facilitate the task of reading the dosage rate at frequent intervals and under all manner of conditions, it is desirable to find some means of dispensing with the microscope.

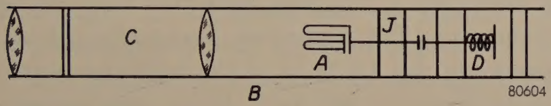

Fig. 1 Simplified diagram of a widely used type of pocket dosemeter. *A* sensitive system, *B* housing, *C* microscope, *D* charging contact and *J* insulator.

With the idea of effecting these improvements C.C. and T. Lauritsen have designed a simple pocket dosemeter with its own charger [3]).

This dosemeter is essentially an electrostatic meter, with the pointer mounted in bearings. It incorporates a charger operating on the principle of friction between two solids, and is approximately the size of a cigarette packet. Although moisture-proof, this instrument is not vacuum-tight, and so contains air at a pressure of 1 atm. It can be used either as a dosemeter, or as a dosage-rate meter.

A new design

A new dosemeter has been designed (*fig. 2*) based on the above considerations but having a vacuum-tight chamber. This allows complete freedom of choice as to the type and pressure of the gas contained in the ionization chamber, and so permits the attainment of a wide variety of sensitivities. Other advantages of this instrument are that it is inexpensive and can conveniently be carried in the pocket.

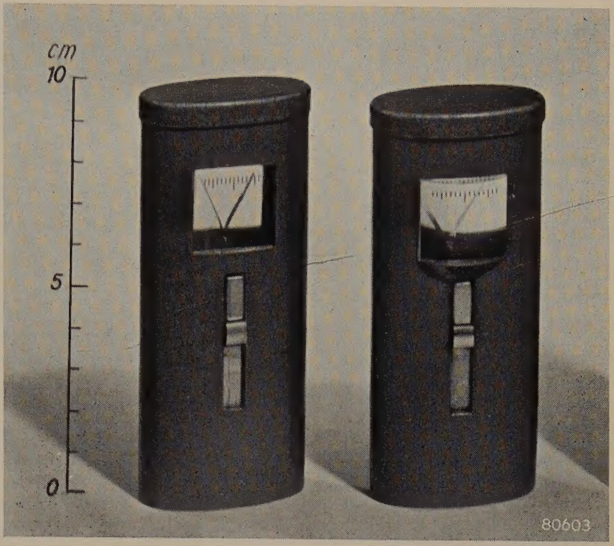

Fig. 2. Pocket dosemeter with built-in charger; the model on the right is fitted with a cylindrical lens window which acts as a magnifier.

The electroscope-system employed comprises two identical, rectangular conductive foils. The material used, besides being easy to trim and mount, is such that it neither sags appreciably under its own weight, nor vibrates unduly when in vacuum. The elasticity of this material must of course be consistent with a reasonable deflection of the system at moderate voltages. One end of the two foils (or leaves) is attached to an efficient insulator in the form of a rod or tube (*fig. 3*). It will be seen that the system as a whole bears a very close resemblance to the old gold-leaf electroscope; in the uncharged condition the leaves are parallel to each other. The electroscope system is housed in an oblong bulb of oval cross-section, made of glass having good conducting properties. This is to prevent the accu-

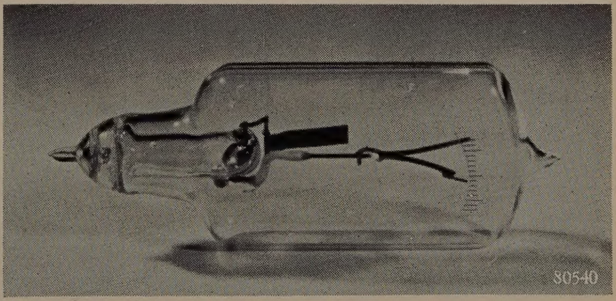

Fig. 3. The electrostatic system of the pocket dosimeter.

---

[3]) C. C. and T. Lauritsen, Science **112**, 137, 1950.

mulation on the bulb wall of charges which would interfere with the measurement. The sensitivity of this instrument is such that 2.5 kV, gives the full scale deflection of about 10 mm.

The insulator is mounted on the end of the charger incorporated in the instrument. The charger is a glass tube some millimetres in diameter and a few centimetres long containing a drop of mercury. When shaken to and fro in the tube, this mercury acquires a charge, which is transferred direct to a contact wire. Also included in the instrument is a switch, which, when in a certain position, establishes electrical contact between the wire in the charger and the sensitive system. When open, the switch is locked to the wall of the bulb by a small magnet, to eliminate the risk of the system being discharged by accidental contact with the charger whilst the instrument is being carried in the pocket. Charger and switch are sealed vacuum-tight into the bulb, so that the latter can be filled with a suitable gas and used, as already described, as an ionization chamber.

The bulb is enclosed in an aluminium or plastic case, which also contains the operating mechanism for the magnetically operated switch mentioned above. Two apertures, one on each side of the case and exactly opposite each other, are provided for reading the electroscope. The electroscope leaves themselves act as the pointers for this reading. A frosted plate on which a scale may be engraved, is fitted in the rear aperture. The scale can alternatively be inserted at the front, but in some models a large cylindrical lens of plastic is fitted in the front aperture. This facilitates reading generally, but also enables the meter to be read from a distance, for example when placed on a laboratory bench as part of an experiment which must be remotely controlled. In normal use the instrument is fixed in the waistcoat or breast pocket by means of a strong clip provided at the back.

To charge the dosemeter, the magnetic switch is pressed down and, if necessary, the flat back of the instrument tapped lightly on the hand to detach the switch from the wall of the bulb, so that it will drop onto the contact connected to the system. The position of the switch is readily visible. Next, the electrometer is shaken fairly vigorously, lengthwise and at an angle of 45° to the horizontal, with the window end held lower than the switch end. The leaves will then be seen to diverge; when they have reached the limit of deflection, the magnet is pushed towards the window, the meter being held in the same slanting position throughout this process.

Once charged, the instrument may be employed either as a dosemeter or as a dosage-rate meter; the variation in deflection during periods when the meter is not exposed to radiation is less than 1% per 24 hours. Shaking-tests have shown that, provided suitable materials are employed, the mercury-drop charger will continue to function almost indefinitely (i.e. after more than 1 million chargings) without any decrease in the voltage generated. During these tests, the complete instrument was shaken very vigourously to test its robustness; this is a quality usually difficult to produce in chargers operating in the principle of friction between two solids, and is important for an instrument which is to be carried in the pocket.

The sensitivity of an ionization chamber is governed primarily by the volume, nature and pressure of the gas filling, and to a lesser extent by the material constituting the wall of the chamber. A suitable choice of all these variables makes it possible to make radiation meters of this type in three distinct and widely different grades of sensitivity, all three being little dependent on the wavelength of the measured radiation. The most sensitive type, tested with the γ-radiation emitted by cobalt 60 (about 1.2 MeV), gives full scale deflection for a dosage of 0.2 röntgens. The sensitivity is not affected by any decrease in the hardness of the radiation until the energy drops to 300 keV; below this energy, the sensitivity increases until, at 150 keV, it reaches a maximum which is twice as high as the value at 1 MeV.(*fig. 4*). A further decrease in hardness to 75 keV restores the sensitivity to its original level; any further softening of the radiation is accompanied by a decrease in sensitivity owing to absorption by the bulb. However, at 50 keV the sensitivity is still about 60% of the original value.

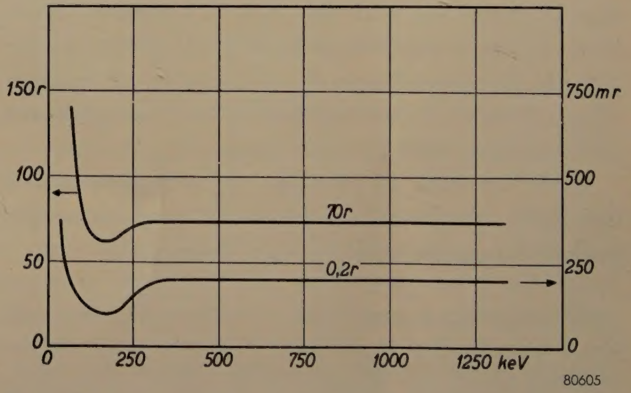

Fig. 4. Variation of full-scale deflection dosage with hardness of radiation, for dosemeters of nominal ranges 0.2 r and 70 r, respectively. (These measurements were carried out in collaboration with Mr. E. Harberink, of the Philips Laboratories in Eindhoven)

This relatively greater sensitivity to soft radiation arises from the fact that is impossible to employ in the dosemeter materials entirely equivalent to air; hence photo-electric X-ray absorption affects the measurements quite appreciably even at 100 - 200 keV.

The most sensitive model just described is designed primarily with a view to the protection of laboratory workers; a weekly tolerance dosage of 0.3 r is well within its range.

In the second model, full scale deflection corresponds to 70 röntgens; it will be seen from fig. 4 that the sensitivity of this particular instrument is governed only very slightly by the wavelength of the incident radiation; the maximum at 150 keV represents a mere 15% increase in sensitivity. This virtual independence of wavelength is obtained by employing a separate, built-in ionization chamber.

The third model covers dosages up to 250 röntgens at full scale deflection. The sensitivity is higher by a factor of about 2 at the maximum than at 1 MeV. By reason of the low pressure and high field intensity employed, the ion current in this model reaches saturation relatively slowly; this may be an advantage, particularly in the measurement of flash dosages. Model three can be adapted for the measurement of still higher dosages.

All these models are insulated so thoroughly that the discharge per month in the absence of radiation is at most one or two percent.

Other applications

Consider now the electrometer without the charger, as shown in *fig. 5*. As in the instrument already described, the whole of the bulb, other than the long neck to which the system is sealed, is made of glass having good conducting properties. The neck has good insulating properties, and is coated with a water-repellant material which enables the system to retain its charge for a long time. Being vacuum-tight, the instrument is not affected by humidity in the surrounding atmosphere. The sensitivity is 2.5 kV at a full scale deflection of 10 scale divisions. A considerable reduction of the sensitivity can be effected by employing thicker leaves. To determine whether an object is charged, it is only necessary to hold the instrument against or near to the object. The electroscope is easily fixed in an apparatus at any point where a measurement of voltage is required. It is therefore very suitable for use in schools and for demonstration purposes: an enlarged image of the system can be very simply projected on to a screen. The charging unit (*fig. 6*) can also be used individually in demonstrations. The long glass tube containing the drop of mercury and a sealed-in contact is best suited to this purpose; it is capable of generating 3 kV. By shaking the charger vigorously, it is possible to produce a current of some tenths of a μA. The other type of charger, fitted with a flexible connection, is suitable for charging the fountain-pen type of pocket dosimeter.

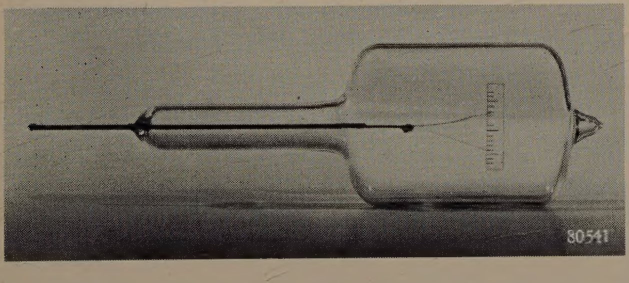

Fig. 5. Electroscope for experimental and educational purposes.

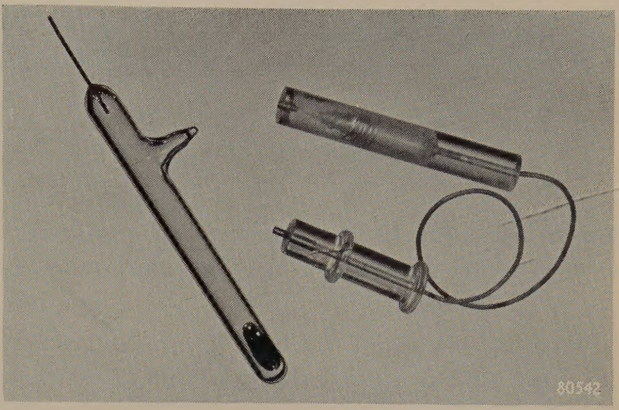

Fig. 6. Two types of mercury friction chargers. The maximum voltage obtainable in the absence of any current leak is about 3 kV.

Summary. Following a brief recapitulation of the effects of ionizing radiations upon biological tissue, the principles of dosimetry, tolerance dosages and the effects of intense irradiation are considered. After descriptions of existing types of pocket dosimeter a more detailed account is given of a new design which incorporates a self-charger and which dispenses with a microscope. This instrument is fully enclosed in a vacuum-tight bulb of conductive glass, which, in turn, is housed in an aluminium case. Full scale deflections corresponding to dosages of 0.2 r, 70 r, 250 r, or more, can be obtained by adopting suitable dimensions for the instrument and by varying the gas pressure. The discharge in the absence of radiation is considerably less than 1% per 24 hours. The charger is a glass tube containing a drop of mercury, which during the charging process, is connected to the sensitive system by means of a magnetic switch. Charging is effected by shaking the instrument several times, with the electrometer system facing downwards. Attention also is drawn to the suitability of the individual electroscope and charger systems for demonstration purposes.

ABSTRACTS OF RECENT SCIENTIFIC PUBLICATIONS OF N.V. PHILIPS' GLOEILAMPENFABRIEKEN

Reprints of these papers not marked with an asterisk * can be obtained free of charge upon application to Philips Electrical Ltd., Century House, Shaftesbury Avenue, London W.C. 2.

2093: K. S. Knol and J. Volger: Is a superconductor free from noise? (Physica **19**, 46-50, 1950, No. 1/2).

From measurements at 6 Mc/s it is concluded that no extra noise is generated in a ring of NbN when this ring is brought into a superconducting state, even when a persisting current of about 100 A is excited.

2094: G. H. Jonker and J. H. van Santen: Magnetic compounds with perovskite structure, III. Ferromagnetic compounds of cobalt (Physica **19**, 120-130, 1953, No. 1/2).

Polycrystalline mixed crystals of $(La,Sr)CoO_3$ have been prepared. Perovskite structure is found for all compositions. Ferromagnetism is observed for medium Sr concentrations. Curves are given for the saturation magnetization, the paramagnetic Curie temperature, and the effective paramagnetic moment as a function of composition. It is suggested that the ferromagnetism observed is caused essentially by a positive Co^{3+}-Co^{4+} interaction. The sign of the exchange interaction is discussed in connection with the theory of Anderson and Polder, and the theory of Zener.

2095: K. H. Klaassens and J. H. Gisolf: Polymerization in bulk at high pressures (J. Polymer Sci. **10**, 140-150, 1953, No. 2).

An apparatus is described for polymerizing monomers in bulk up to a pressure of 10 000 atmospheres, in which the polymerizing substance can be heated and the temperature of the substance measured. Styrene shows an explosive reaction at 10 000 atmospheres and at about 70 °C. Indene polymerizes slowly when heated at 10 000 atmospheres and shows an explosive reaction at 175 °C. Both compounds give a solid polymer. Croton aldehyde heated at 10 000 atmospheres gives a brittle, high-melting polymer. Coumarone and some chlorinated ethylenes carbonize when heated at 10 000 atmospheres. Butyraldehyde polymerizes to a solid product which rapidly reverts to the monomer.

2096: J. I. de Jong and J. de Jonge: The hydrolysis of methylene diurea (Rec. Trav. chim. Pays-Bas **72**, 202-206, 1953, No. 3).

The hydrolysis of methylene diurea giving urea and monomethylolurea was found to be a monomolecular reaction. The rate of the reaction is directly proportional to the hydrogen ion concentration in the *pH* range measured (3-5) and independent of the buffer concentration. The activation energy appears to be 19.5 kcal/mole. Generally, the reaction of an amidomethylol group with an amide group leading to the formation of a methylene bridge between urea fragments, will be a reversible reaction. The rates of both the forward and the reverse reactions are proportional to the hydrogen ion concentration.

2097: J. I. de Jong and J. de Jonge: Kinetics of the reaction between monomethylolurea and methylene diurea (Rec. Trav. chim. Pays-Bas **72**, 207-212, 1953, No. 3).

The reaction between monomethylolurea and methylene diurea appears to be bimolecular, and the rate constants were found to be directly proportional to the concentration of the hydrogen ions. An influence of the buffer concentration was not observed. The activation energy was found to be 15 kcal/mole.

2098: J. I. de Jong and J. de Jonge: The reaction of methylene diurea with formaldehyde (Rec. Trav. chim. Pays-Bas **72**, 213-217, 1953, No. 3).

The reaction of methylene diurea with formaldehyde shows a close resemblance to the previously studied reaction of urea and formaldehyde (see these abstracts, No. **2046**) i.e. the reaction proved to be bimolecular and the rates were found to be directly proportional to the concentration of hydrogen ions; an influence of the buffer concentration on the rate was also observed. Obviously the reaction is subject to general acid and/or base catalysis. The activation energy appeared to be about 15 kcal/mole. The values for the rate constants were almost the same as were found for the reaction between urea and formaldehyde.